Supplementary Information

Foldameric Receptors with Domain-Swapping Cavities Capable of Selectively Binding and Transporting Monosaccharides

Geunmoo Song , Seungwon Lee and Kyu-Sung Jeong*

*Department of Chemistry, Yonsei University, Seoul 03722, Korea

Fax: +82-2-364-7050

Tel: +82-2123-2643

E-mail: ksjeong@yonsei.ac.kr

Contents

General method: All chemicals were purchased from commercial suppliers and used without further purification unless otherwise specified. Dichloromethane (CH_2Cl_2) were purified by drying over calcium hydride (CaH_2), followed by distillation. Ethyl acetate (EtOAc) and acetone were distilled. Thin layer chromatography (TLC) was performed on Merck (silica gel 60, F-254, 0.25 mm). Silica gel 60 (230-400 mesh, Merck) was used for column chromatography. Melting points were determined with a Barnstead Electrothermal (IA9100) apparatus. NMR spectra were measured by using Bruker DRX 400, Avance II instruments. Abbreviations used when describing NMR spectra are as follows: s, singlet; d, doublet; dd, doublet of doublet; t, triplet; m, multiplet. Coupling constants (*J*) are given in Hz. Chemical shifts are reported using residual protonated solvent peaks (for ^{1}H NMR spectra, DMSO-d_6 2.50 ppm; Acetone-d_6 2.05 ppm; CD_2Cl_2 5.32 ppm; $CDCl_3$ 7.32 ppm and for ^{13}C NMR spectra, DMSO-d_6 39.5 ppm; Acetone-d_6 29.8 ppm; CD_2Cl_2 53.8 ppm $CDCl_3$ 77.2 ppm). NMR data processing was achieved with Topspin 4.1.1 software. ESI-HRMS spectrometric measurements were obtained from the National Instrument Center for Environmental Mangement at Seoul National University. MALDI-TOF-HRMS spectra were recorded on a Bruker Autoflex Max MALDI-TOF/TOF MS (Bruker Daltonics, Bremen, Germany). Energy-minimized structures were obtained using *MacroModel 9.1 program* with MMFFs force field in $CHCl_3$ phase.

1. Syntheses and characterisation of new compounds

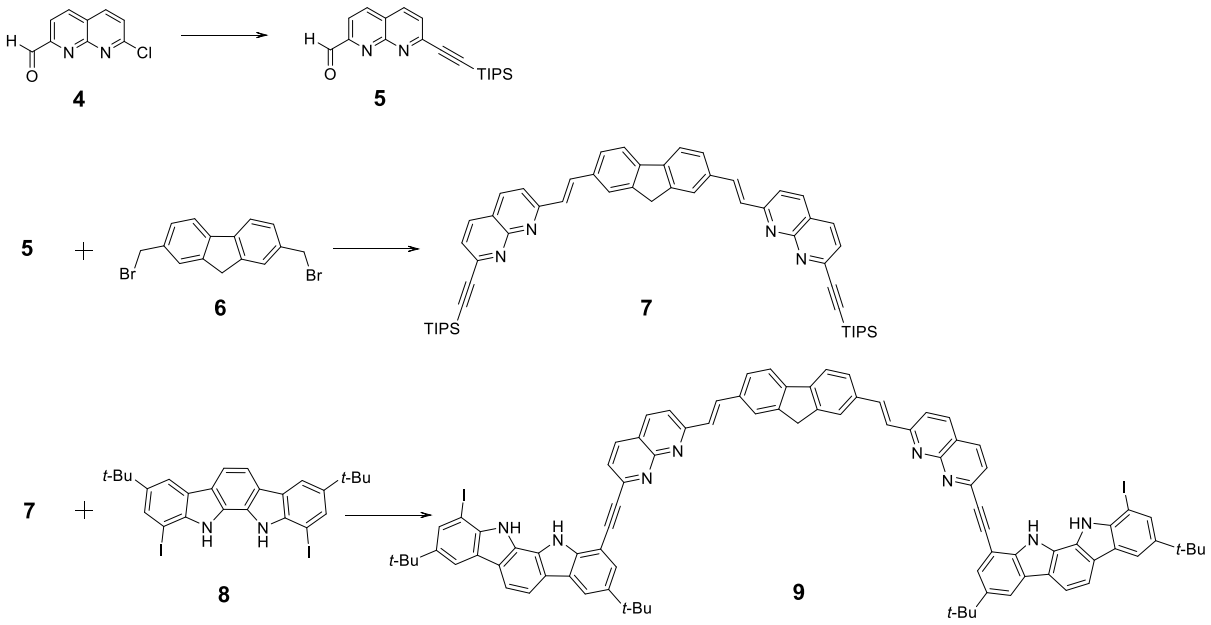

5: A Schlenk flask containing **4**[S1] (220 mg, 1.14 mmol), CuI (6.5 mg, 0.034 mmol) and $Pd(PPh_3)_2Cl_2$ (24 mg, 0.034 mmol) was evacuated under vacuum and back-filled with nitrogen. Anhydrous, degassed tetrahydrofuran (THF) (4.0mL), triethylamine (Et_3N) (0.6 mL), and (triisopropylsilyl)acetylene (0.5 mL, 2.28 mmol) were sequentially added and the solution was stirred at 55 ℃ for 3.5 h. The reaction mixture was cooled to room temperature, filtered through

Celite with CH_2Cl_2 and concentrated. The residue was dissolved in CH_2Cl_2, washed with brine, and dried over anhydrous Na_2SO_4. The residue was concentrated and purified by flash column chromatography (silica gel, hexanes:CH_2Cl_2:ethyl acetate (EtOAc)= 1:1:0.2 (v/v/v)) to give compound **5** (200 mg, 52 %) as a grey solid; mp > 160 ℃ (dec); ^{1}H NMR (400 MHz, Acetone-d_6, 25 ℃, ppm) δ 10.18 (d, J = 0.9 Hz, 1H), 8.68 (dd, J = 8.3 Hz, 0.9 Hz, 1H), 8.58 (d, J = 8.4 Hz, 1H), 8.09 (d, J = 8.3 Hz, 1H), 7.87 (d, J = 8.4 Hz, 1H), 1.23–1.08 (m, 21H); ^{13}C NMR (100 MHz, Acetone-d_6, 25 ℃, ppm) δ 194.1, 156.5, 156.4, 148.2, 140.2, 139.0, 128.1, 125.6, 118.9, 107.2, 94.9, 18.9, 11.9; ESI-HRMS, m/z calcd for $C_{20}H_{26}N_2OSi$ $[M+H]^+$ 339.1887 found 339.1890

7: A round bottom flask containing **6**[S2] (76 mg, 0.216 mmol), triphenylphosphin (141 mg, 0.54 mmol) and NaH (24 mg, 0.45 mmol) was evacuated under vacuum and back-filled with nitrogen. Anhydrous dimethylformamide (DMF) was added and the solution as stirred at 40 ℃. After 30 min, **5** (146 mg, 0.43 mmol) was added and stirred for 4h. The reaction mixture was cooled to room temperature, diluted through ethyl acetate, and washed with brine. After dried over anhydrous Na_2SO_4, the residue was concentrated and purified by flash column chromatography (silica gel, hexanes:CH_2Cl_2:tetrahydrofuran (THF) = 4:4:1 (v/v/v)) to give compound **7** (80 mg, 44 %) as a yellow solid; mp > 225 ℃ (dec); ^{1}H NMR (400 MHz, Acetone-d_6, 25 ℃, ppm) δ 8.39 (d, J = 8.3 Hz, 1H), 8.38 (d, J = 8.3 Hz, 1H), 8.12 (d, J = 16.1 Hz, 1H), 8.00 (s, 1H), 7.97 (d, J = 8.1 Hz, 1H), 7.87 (d, J = 8.1 Hz, 1H), 7.82 (d, J = 8.2 Hz, 1H), 7.67 (d, J = 8.1 Hz, 1H), 7.57 (d, J = 16.2 Hz, 1H), 4.05 (s, 1H), 1.23–1.20 (m, 21H); ^{13}C NMR (100 MHz, $CDCl_3$, 25 ℃, ppm) δ 159.8, 156.1, 147.1, 144.6, 142.5, 137.1, 136.9, 136.6, 135.5, 127.3, 127.2, 125.4, 124.1, 121.9, 121.3, 120.6, 106.4, 94.7, 18.7, 11.5; ESI-HRMS, m/z calcd for $C_{55}H_{62}N_4Si_2$ $[M+H]^+$ 835.4586 found 835.4593

9: A Schlenk flask containing **7** (53 mg, 0.063 mmol), **8**[S3] (305 mg, 0.51 mmol), CuI (1.2 mg, 0.006 mmol), and $Pd(PPh_3)_2Cl_2$ (4.4 mg, 0.006 mmol) was evacuated under vacuum and back-filled with nitrogen. Anhydrous, degassed dimethylformamide (DMF) (1.2 mL), triethylamine (Et_3N) (0.2 mL), and tetrabutylammonium fluoride (0.14 mL, 1.0 M solution in THF) were sequentially added, and the solution was stirred at 45 ℃ for 2.5 h. The mixture was cooled to room temperature, filtered through Celite with THF, and concentrated. The residue was dissolved in ethyl acetate, washed with brine, and dried over anhydrous Na_2SO_4. After concentrated, the residue was purified by flash column chromatography (silica gel, hexanes : THF : MeOH : TEA = 10:10:1:1 (v/v/v/v)) to give compound **9** (59 mg, 62 %) as a yellow

solid; mp > 240 ℃ (dec); ^{1}H NMR (400 MHz, DMSO-d_6, 25 ℃, ppm) δ 11.49 (s, NH, 1H), 11.13 (s, NH, 1H), 8.56 (d, J = 8.2 Hz, 1H), 8.53 (d, J = 8.3 Hz, 1H), 8.40 (d, J = 1.4 Hz, 1H), 8.24 (s, 1H), 8.12 (d, J = 16.1 Hz, 1H), 8.09–7.99 (m, 6H), 7.86 (d, J = 8.3 Hz, 1H), 7.83 (d, J = 1.3 Hz, 1H), 7.82 (d, J = 1.3 Hz, 1H), 7.66 (d, J = 16.2 Hz, 1H), 4.13(s, 1H), 1.49 (s, *t*-Bu, 9H), 1.43 (s, *t*-Bu, 9H); ^{13}C NMR (100 MHz, DMSO-d_6, 25 ℃, ppm) δ 159.5, 155.6, 146.0, 144.4, 143.9, 142.2, 141.8, 139.1, 137.8, 135.1, 130.7, 128.8, 127.8, 127.2, 126.3, 125.9, 125.5, 124.0, 123.8, 121.2, 121.1, 120.4, 118.9, 116.3, 112.7, 112.4, 103.0, 93.2, 88.1, 83.7, 76.7, 72.2, 60.2, 34.6, 34.4, 31.8, 31.7; MALDI-TOF-HRMS, m/z calcd for $C_{89}H_{72}I_2N_8$ $[M+H]^+$ 1507.4042 found 1507.4029

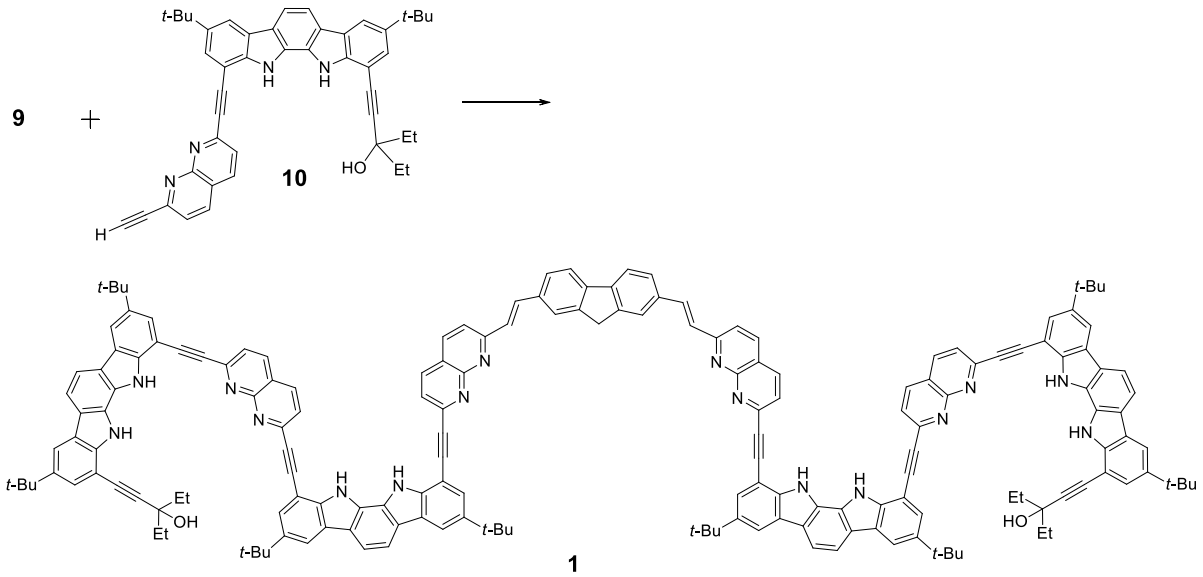

1: A Schlenk flask containing **9** (80 mg, 0.053 mmol), **10**[S4] (76 mg, 0.12 mmol), CuI (1.0 mg, 0.0053 mmol), and $Pd(PPh_3)_2Cl_2$ (3.7 mg, 0.0053 mmol) was evacuated under vacuum and back-filled with nitrogen. Anhydrous, degassed dimethylformamide (DMF) (1.0 mL), and triethylamine (Et_3N) (0.1 mL) were sequentially added, and the solution was stirred at 45 ℃ for 2.5 h. The mixture was cooled to room temperature, filtered through Celite with CH_2Cl_2, and concentrated. The residue was dissolved in ethyl acetate, washed with brine, and dried over anhydrous Na_2SO_4. After concentrated, the residue was purified by flash column chromatography (silica gel, hexanes : THF : MeOH : TEA = 10:10:1:1 (v/v/v/v)) to give compound **1** (71 mg, 52 %) as a yellow solid; mp > 275 ℃ (dec); ^{1}H NMR (400 MHz, DMSO-d_6, 25 ℃, ppm) δ 11.63 (s, 1H), 11.45 (s, 1H), 11.38 (s, 1H), 10.74 (s, 1H), 8.57 (d, J = 8.4 Hz, 1H), 8.45 (s, 1H), 8.43 (s, 1H), 8.35 (d, J = 1.4 Hz, 1H), 8.35 (d, J = 8.3 Hz, 1H), 8.18 (d, J = 1.4 Hz, 1H), 8.14 (s, 4H), 8.01 (d, J = 8.3 Hz, 1H), 7.96 (d, J = 8.4 Hz, 1H), 7.88 (d, J = 8.3

Hz, 1H), 7.94 (d, *J* = 1.5 Hz, 1H), 7.82 (s, 1H), 7.80 (d, *J* = 7.5 Hz, 1H), 7.79 (d, *J* = 8.3 Hz, 1H), 7.76 (d, *J* = 8.2 Hz, 1H), 7.68 (d, *J* = 16.1 Hz, 1H), 7.66 (d, *J* = 1.4 Hz, 1H), 7.63 (s, 1H), 7.45 (d, *J* = 7.5 Hz, 1H), 7.43 (d, *J* = 1.6 Hz, 1H), 7.31 (d, *J* = 8.3 Hz, 1H), 7.21 (d, *J* = 16.2 Hz, 1H), 5.18 (s, OH), 3.70 (s, 1H), 1.75–1.62 (m, 4H), 1.50 (s, 18H, *t*-Bu), 1.44 (s, 9H, *t*-Bu), 1.38 (s, 9H, *t*-Bu), 0.98 (t, *J* = 7.3 Hz, 6H); ^{13}C NMR (100 MHz, DMSO-d_6, 25 ℃, ppm) δ 158.9, 155.3, 155.2, 146.7, 145.7, 143.9, 142.2, 142.1, 141.8, 141.7, 141.5, 138.0, 137.9, 137.8, 137.1, 134.7, 127.1, 126.3, 126.0, 125.9, 125.9, 125.8, 125.7, 124.2, 124.1, 123.7, 121.2, 120.8, 120.7, 120.6, 120.4,, 119.1, 118.8, 116.7, 112.5, 112.3, 112.1, 105.0, 103.2, 102.9, 97.5, 93.2, 93.1, 92.9, 89.4, 89.0, 87.9, 79.7, 70.9, 34.5, 34.4, 34.3, 33.8, 31.7, 31.6, 29.0, 20.7, 8.7; ESI-HRMS, m/z calcd for $C_{179}H_{154}N_{16}O_2$ $[M+2H]^{2+}$ 1280.6293 found 1280.6277

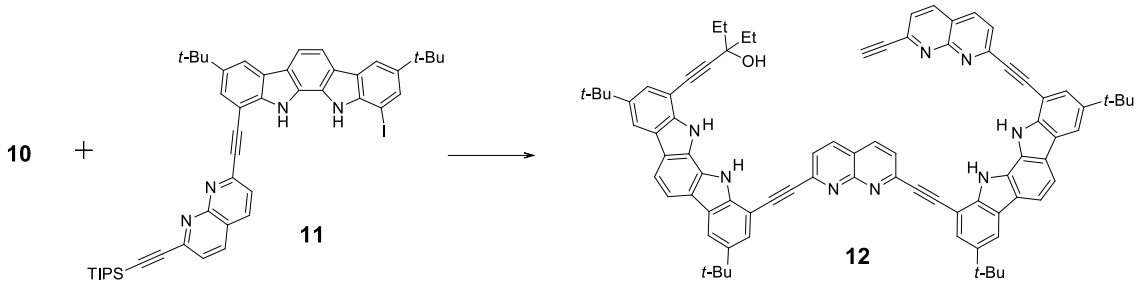

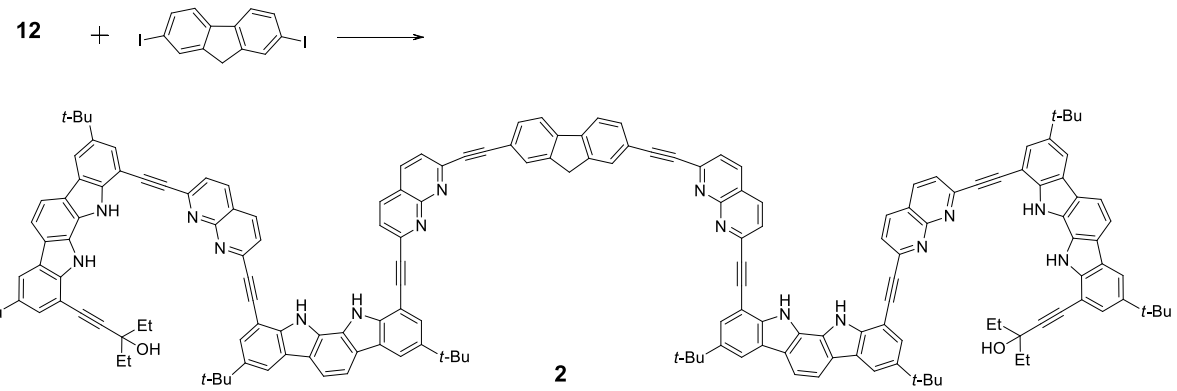

12: A Schlenk flask containing **10** (300 mg, 0.46 mmol), **11**[S5] (380 mg, 0.46 mmol), CuI (4.4 mg, 0.023 mmol), and $Pd(PPh_3)_2Cl_2$ (16 mg, 0.023 mmol) was evacuated under vacuum and back-filled with nitrogen. Anhydrous, degassed dimethylformamide (DMF) (3.0 mL), and triethylamine (Et_3N) (0.26 mL) were sequentially added, and the solution was stirred at 45 ℃ for 3 h. The mixture was cooled to room temperature, filtered through Celite with CH_2Cl_2, and concentrated. The residue was dissolved in ethyl acetate, washed with brine, and dried over anhydrous Na_2SO_4. After concentrated, the residue was dissolved in THF (6 mL) and added dropwise TBAF (0.6 mL, 1.0 M solution in THF). After 30 min stirring in room temperature,

the residue was concentrated and purified by flash column chromatography (silica gel, CH_2Cl_2 : MeOH = 50:1 (v/v)) to give compound **12** (450 mg, 81 %) as a yellow solid; mp > 214 ℃ (dec); ^{1}H NMR (400 MHz, DMSO-d_6, 25 ℃, ppm) δ 11.56 (s, 1H), 11.53 (s, 1H), 11.46 (s, 1H), 10.88 (s, 1H), 8.70 (d, J = 8.4 Hz, 1H), 8.69 (d, J = 8.3 Hz, 1H), 8.44 (s, 1H), 8.43 (s, , 2H), 8.39 (d, J = 8.4 Hz, 1H), 8.24 (s, 1H), 8.18 (d, J = 8.2 Hz, 1H), 8.15 (d, J = 8.1 Hz, 1H), 8.13 (d, J = 8.0 Hz, 1H), 8.12 (s, 2H), 8.08 (d, J = 8.2 Hz, 1H), 8.05 (d, J = 8.2 Hz, 1H), 8.00 (d, J = 8.3 Hz, 1H), 7.83 (s, 1H), 7.81 (s, 2H), 7.47 (d, J = 8.1 Hz, 1H), 7.45 (d, J = 1.4 Hz, 1H), 5.26 (s, 1H), 4.58 (s, 1H), 1.77–1.67 (m, 4H), 1.50 (s, 9H, *t*-Bu), 1.48 (s, 18H, *t*-Bu), 1.42 (s, 9H, *t*-Bu), 1.01 (t, J = 7.5 Hz, 6H); ^{13}C NMR (100 MHz, DMSO-d_6, 25 ℃, ppm) δ 155.4, 154.9, 146.8, 146.7, 146.6, 145.7, 142.2, 142.1, 141.8, 138.2, 138.0, 137.9, 137.9, 137.8, 137.2, 126.4, 126.2, 126.1, 126.0, 125.9, 125.7, 125.3, 124.2, 124.1, 123.7, 121.5, 121.4, 120.8, 120.7, 120.5, 119.0, 119.0, 116.8, 112.5, 112.4, 112.2, 105.0, 102.9, 102.8, 97.6, 93.0, 93.0, 92.8, 89.3, 89.1, 88.8, 83.0, 82.6, 79.6, 70.9, 37.6, 34.6, 34.4,33.8, 31.7, 17.8, 12.0, 8.7; ESI-HRMS, m/z calcd for $C_{83}H_{72}N_8O$ $[M+H]^+$ 1197.5902 found 1197.5916

2: A Schlenk flask containing **12** (292 mg, 0.244 mmol), 2,7-diiodo-9H-fluorene (49 mg, 0.116 mmol), CuI (2.2 mg, 0.0116 mmol), and $Pd(PPh_3)_2Cl_2$ (8.1 mg, 0.0116 mmol) was evacuated under vacuum and back-filled with nitrogen. Anhydrous, degassed dimethylformamide (DMF) (1.5 mL), and triethylamine (Et_3N) (0.2 mL) were sequentially added, and the solution was stirred at 45 ℃ for 3.5 h. The mixture was cooled to room temperature, filtered through Celite with CH_2Cl_2, and concentrated. The residue was dissolved in ethyl acetate, washed with brine, and dried over anhydrous Na_2SO_4. After concentrated, the residue was purified by flash column chromatography (silica gel, hexanes : CH_2Cl_2 : THF = 4:4:1 (v/v/v)) to give compound **2** (160 mg, 54 %) as a yellow solid; mp > 265 ℃ (dec); ^{1}H NMR (400 MHz, DMSO-d_6, 25 ℃, ppm) δ 11.56 (s, 1H), 11.44 (s, 2H), 10.78 (s, 1H), 8.61 (d, J = 8.4 Hz, 1H), 8.47 (d, J = 8.4 Hz, 1H), 8.43 (s, 1H), 8.42 (s, 1H), 8.38 (d, J = 1.5 Hz, 1H), 8.21 (d, J = 8.4 Hz, 1H), 8.18 (d, J = 1.6 Hz, 1H), 8.11 (d, J = 8.4 Hz, 1H), 8.47 (s, , 2H), 8.04 (d, J = 8.3 Hz, 1H), 7.98 (d, J = 8.3 Hz, 1H), 7.98 (d, J = 8.3 Hz, 1H), 7.89 (d, J = 8.3 Hz, 1H), 7.86 (d, J = 8.3 Hz, 1H), 7.83 (d, J = 7.5 Hz, 1H), 7.83 (d, J = 1.5 Hz, 1H), 7.81 (d, J = 1.6 Hz, 1H), 7.72 (d, J = 1.6 Hz, 1H), 7.66 (s, 1H), 7.44 (d, J = 1.6 Hz, 1H), 7.42 (d, J = 7.5 Hz, 1H), 7.29 (d, J = 8.3 Hz, 1H), 5.21 (s, OH), 3.78 (s, 1H), 1.76–1.64 (m, 4H), 1.49 (s, 18H, *t*-Bu), 1.43 (s, 9H, *t*-Bu), 1.37 (s, 9H, *t*-Bu), 1.00 (t, J = 7.3 Hz, 6H) ; ^{13}C NMR (100 MHz, DMSO-d_6, 25 ℃, ppm) δ 155.8, 155.5, 147.3, 147.2, 146.9, 146.7, 144.2, 142.7, 142.6, 142.4, 142.2, 142.0, 138.6, 138.4, 138.4, 138.3,

138.2, 137.9, 137.6, 131.4, 129.0, 126.9, 126.5, 126.4, 126.4, 126.2, 125.5, 124.7, 124.6, 124.6, 124.2, 121.8, 121.4, 121.3, 121.2, 121.1, 120.9, 120.0, 119.5, 119.4, 117.2, 113.1, 112.8, 112.6, 105.4, 103.4, 103.4, 103.3, 98.0, 93.6, 93.4, 92.1, 90.1, 90.0, 89.5, 89.3, 80.1, 71.4, 35.0, 34.9, 34.8, 34.3, 33.7, 32.2, 32.1, 23.1, 15.2, 9.2; ESI-HRMS, m/z calcd for $C_{179}H_{150}N_{16}O_2$ $[M+2H]^{2+}$ 1278.6137 found 1278.6130

2. ^{1}H NMR studies

2.1 ^{1}H NMR spectra of receptors **1** and **2** in the presence of various guests

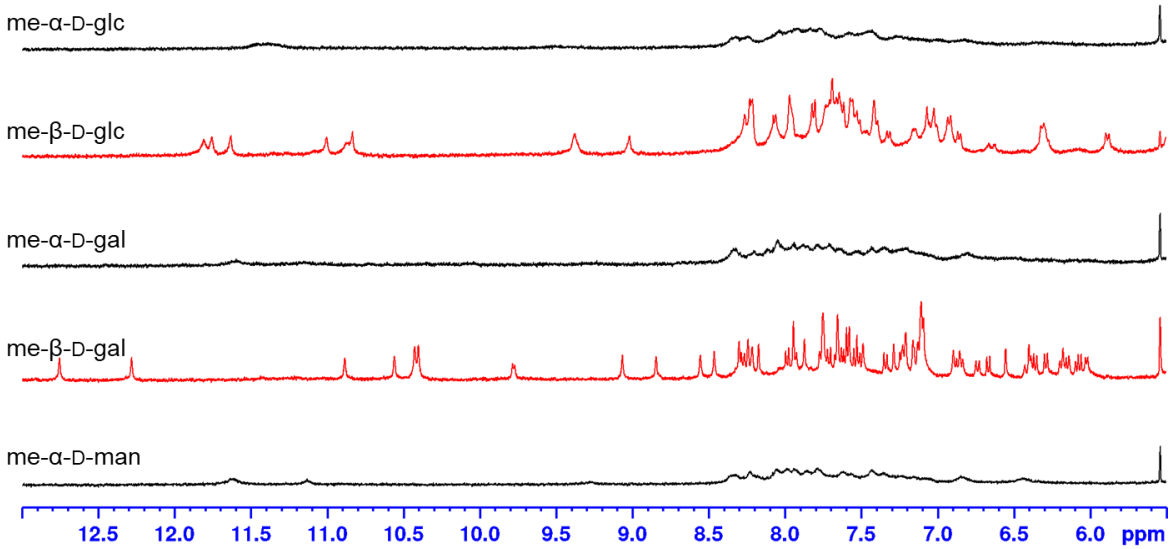

Fig. S1 Partial ^{1}H NMR spectra (400 MHz, 25 ℃) of receptor **1** in the presence of various guests (2.0 equiv of each guest) in 5% (v/v) DMSO-d_6/CD_2Cl_2 (containing ca. 0.05 % water).

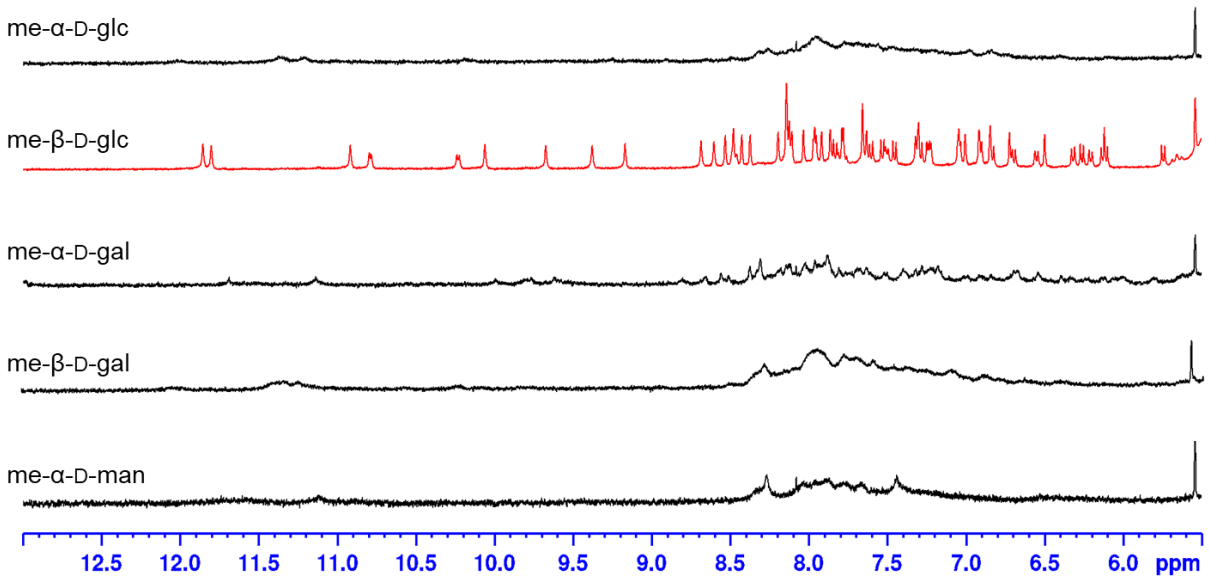

Fig. S2 Partial ^{1}H NMR spectra (400 MHz, 25 ℃) of receptor **2** in the presence of various guests (2.0 equiv of each guest) in 5% (v/v) DMSO-d_6/CD_2Cl_2 (containing ca. 0.05 % water).

2.2 ^{1}H NMR spectra of **1**, (**1**-*MM*)$_2$⊃(me-β-D-gal·2H$_2$O)$_2$, and (**1**-*MP*)$_2$⊃(me-β-D-glc)$_2$

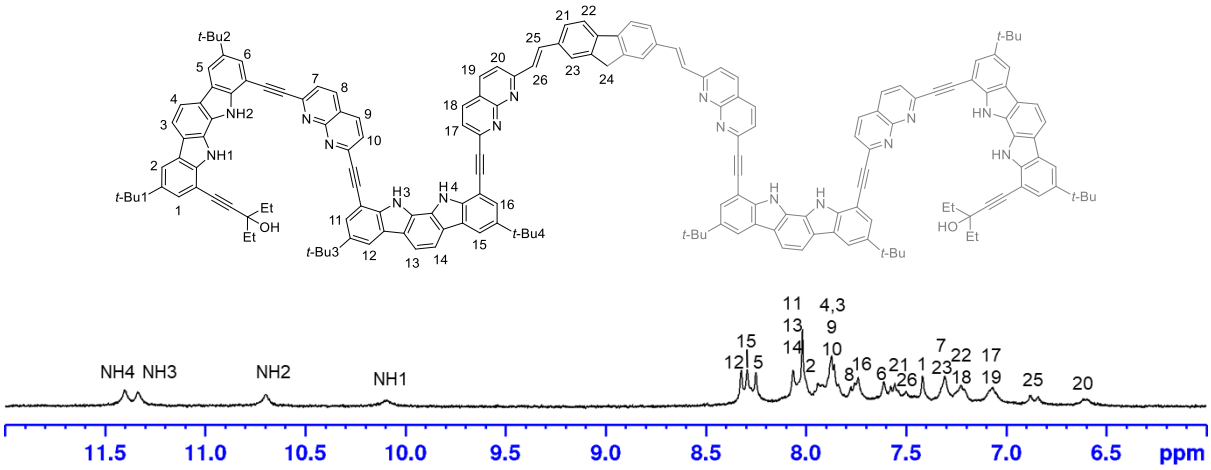

Fig. S3 Partial ^{1}H NMR spectrum (400 MHz, 25 °C) of **1** (2 mM) in 5% (v/v) DMSO-d_6/CD_2Cl_2.

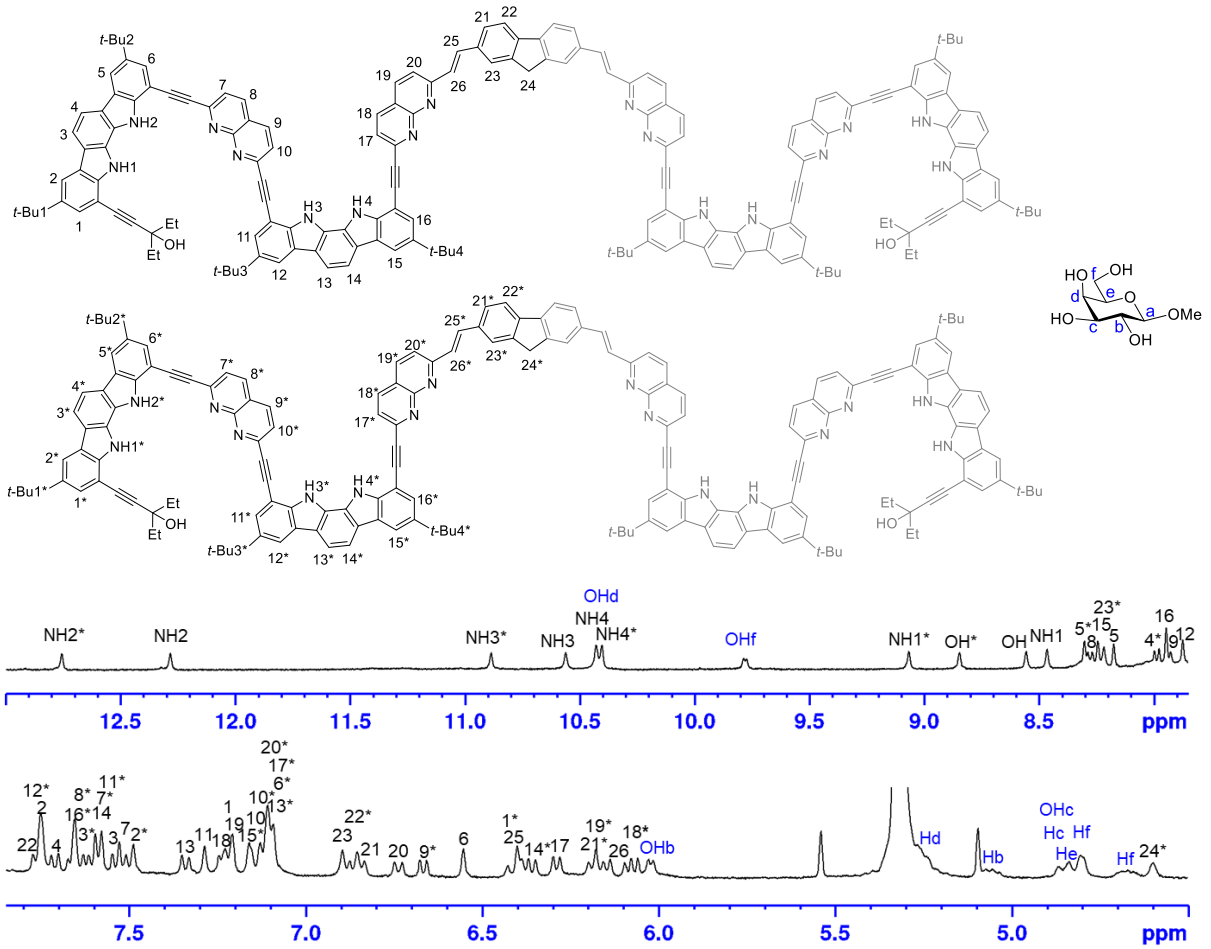

Fig. S4 Partial ^{1}H NMR spectrum (400 MHz, 25 °C) of (**1**-*MM*)$_2$⊃(me-β-D-gal·2H$_2$O)$_2$ (2 mM) in 5% (v/v) DMSO-d_6/CD_2Cl_2. Me-β-D-gal signals are depicted in blue.

Table S1 ^{1}H NMR chemical shifts (400 MHz, 25 °C) of (**1**-*MM*)$_2$⊃(me-β-D-gal·2H$_2$O)$_2$ in 5% (v/v) DMSO-d_6/CD_2Cl_2 and their differences between free **1**.

(**1**-*MM*)$_2$⊃(me-β-D-gal·2H$_2$O)$_2$			(**1**-*MM*)$_2$⊃(me-β-D-gal·2H$_2$O)$_2$		
atom	δ (ppm)	δ (free) − δ (complex)	atom	δ (ppm)	δ (free) − δ (complex)
1	7.24 (d, J = 1.4 Hz)	0.18	1*	6.43 (d, J = 1.5 Hz)	0.99
2	7.76 (d, J = 1.5 Hz)	0.16	2*	7.51 (d, J = 1.5 Hz)	0.41
3	7.55 (d, J = 8.1 Hz)	0.32	3*	7.66 (d, J = 8.0 Hz)	0.21
4	7.73 (d, J = 7.9 Hz)	0.14	4*	8.00 (d, J = 8.0 Hz)	-0.13
5	8.19 (d, J = 1.4 Hz)	0.06	5*	8.31 (d, J = 1.6 Hz)	-0.06
6	6.56 (d, J = 1.4 Hz)	1.05	6*	7.10 (s)	0.51
7	7.54 (d, J = 8.2 Hz)	-0.24	7*	7.61 (d, J = 7.9 Hz)	-0.31
8	8.29 (d, J = 8.1 Hz)	-0.53	8*	7.68 (d, J = 7.9 Hz)	0.08
9	7.96 (d, J = 8.1 Hz)	-0.11	9*	6.67 (d, J = 8.0 Hz)	1.18
10	7.15 (d, J = 7.9 Hz)	0.70	10*	7.14 (d, J = 8.2 Hz)	0.71
11	7.31 (s)	0.71	11*	7.60 (s)	0.42
12	7.89 (d, J = 1.4 Hz)	0.43	12*	7.77 (d, J = 1.6 Hz)	0.55
13	7.36 (d, J = 8.1 Hz)	0.66	13*	7.11 (d, J = 8.0 Hz)	0.91
14	7.62 (d, J = 8.1 Hz)	0.40	14*	6.37 (d, J = 8.0 Hz)	1.65
15	8.26 (d, J = 1.5 Hz)	0.03	15*	7.18 (d, J = 1.4 Hz)	1.11
16	7.97 (d, J = 1.5 Hz)	-0.23	16*	7.68 (d, J = 1.7 Hz)	0.06
17	6.31 (d, J = 7.9 Hz)	0.75	17*	7.11 (d, J = 7.8 Hz)	-0.05
18	7.25 (d, J = 7.9 Hz)	-0.03	18*	6.09 (d, J = 8.0 Hz)	1.13
19	7.23 (d, J = 8.2 Hz)	-0.17	19*	6.19 (d, J = 8.0 Hz)	0.87
20	6.76 (d, J = 8.6 Hz)	-0.14	20*	7.11 (d, J = 8.2 Hz)	-0.49
21	6.86 (d, J = 7.8 Hz)	0.70	21*	6.21 (d, J = 7.4 Hz)	1.35
22	7.78 (d, J = 8.0 Hz)	-0.56	22*	6.89 (d, J = 7.9 Hz)	0.33
23	6.91 (s)	0.39	23*	8.25 (s)	-0.95
24	3.84 (s)	-0.36	24*	4.63 (s)	-1.15
25	6.42 (d, J = 16.5 Hz)	0.44	26	6.13 (d, J = 16.5 Hz)	1.40
OMe	2.41 (s)		Ha	2.93 (d, J = 8.0 Hz)	
OHb	6.08 (d, J = 5.6 Hz)		Hb	5.08	
OHc	4.85		Hc	4.88	
OHd	10.48 (d, J = 6.2 Hz)		Hd	5.27	
OHf	9.83 (d, J = 5. Hz)		He	4.85	
Hf	4.84		Hf	4.68	

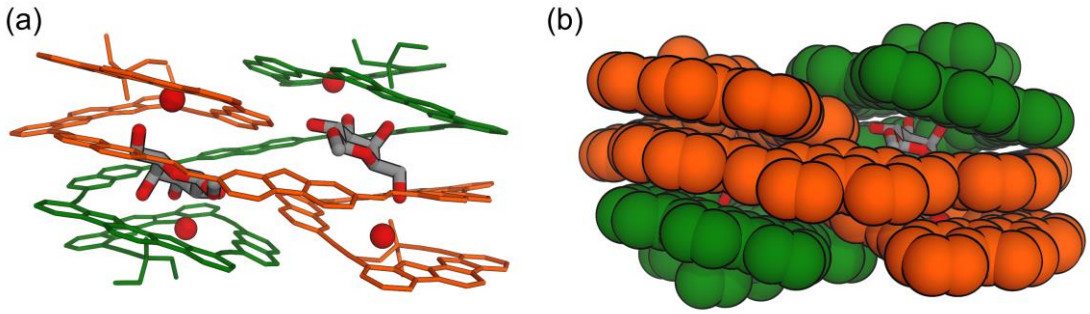

Fig. S5 (a) Tube and (b) space-filling representations of energy-minimized structure of (**1**-*MM*)$_2$⊃(me-β-D-gal·2H$_2$O)$_2$ (MacroModel 9.1, MMFFs force field, $CHCl_3$ phase).

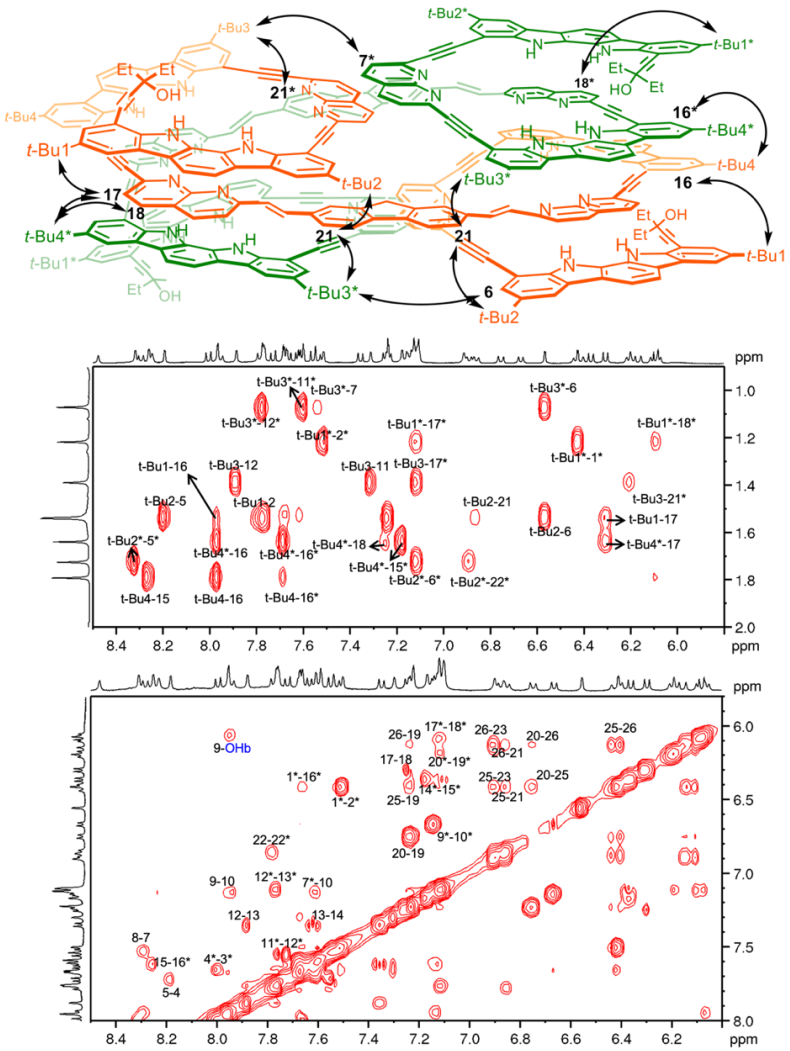

Fig. S6 Partial ^{1}H-^{1}H ROESY spectrum (400 MHz, 25 °C, mixing time: 400 ms) of (**1**-*MM*)$_2$⊃(me-β-D-gal·2H$_2$O)$_2$ (4.0 mM) in 2% (v/v) DMSO-d_6/CD_2Cl_2.

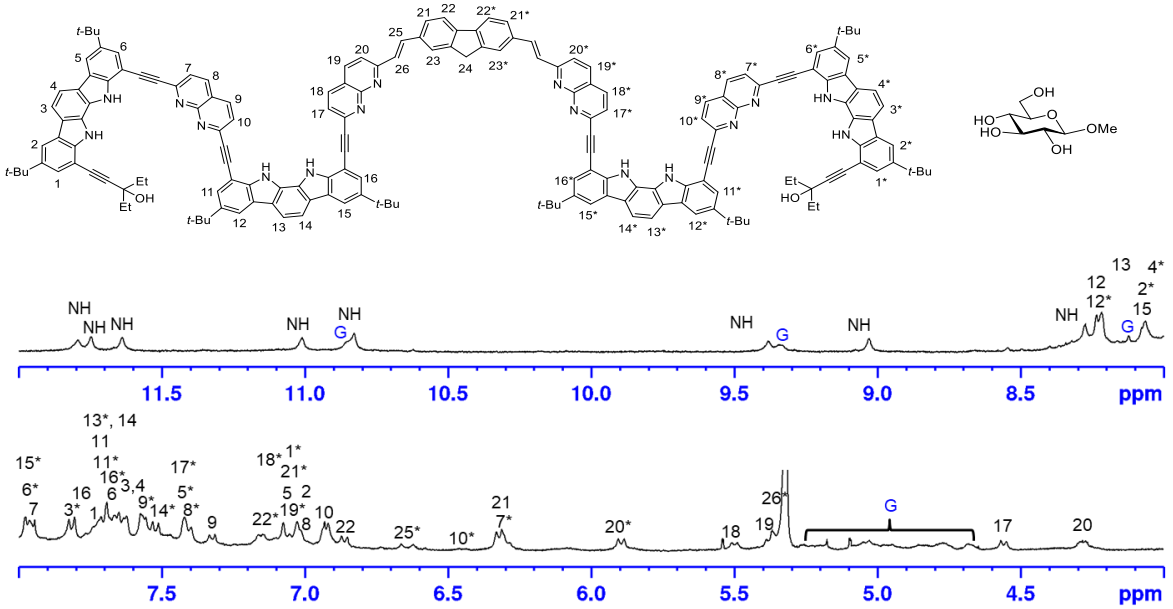

Fig. S7 Partial ^{1}H NMR spectrum (400 MHz, 25 °C) of (**1**-*MP*)$_2$⊃(me-β-D-glc)$_2$ (2 mM) in 5% (v/v) DMSO-d_6/CD_2Cl_2. Me-β-D-glc signals are depicted in blue G.

Table S2 ^{1}H NMR chemical shifts (400 MHz, 25 °C) of (**1**-*MP*)$_2$⊃(me-β-D-glc)$_2$ in 5% (v/v) DMSO-d_6/CD_2Cl_2 and their differences between free **1**.

(**1**-*MP*)$_2$⊃(me-β-D-glc)$_2$			(**1**-*MP*)$_2$⊃(me-β-D-glc)$_2$		
atom	δ (ppm)	δ (free) – δ (complex)	atom	δ (ppm)	δ (free) – δ (complex)
1	7.65 (s)	-0.23	1*	7.05 (s)	0.37
2	7.00 (s)	0.92	2*	8.05 (s)	-0.13
3	7.60	0.27	3*	7.82 (d, J = 8.1 Hz)	0.05
4	7.60	0.27	4*	8.03	-0.16
5	7.10 (s)	1.15	5*	7.40 (s)	0.85
6	7.70 (s)	-0.09	6*	7.95 (s)	-0.34
7	7.95	-0.65	7*	6.35 (d, J = 8.2 Hz)	0.95
8	7.05 (d, J = 8.1 Hz)	0.71	8*	7.38 (d, J = 8.0 Hz)	0.38
9	7.33 (d, J = 8.0 Hz)	0.52	9*	7.55 (d, J = 8.1 Hz)	0.3
10	6.95 (d, J = 8.1 Hz)	0.9	10*	6.45	1.4
11	7.70	0.32	11*	7.70	0.32
12	8.25 (s)	0.07	12*	8.25 (s)	0.07
13	8.15	-0.13	13*	7.75	0.27
14	7.75	0.27	14*	7.55 (d, J = 8.1 Hz)	0.47
15	8.05 (s)	0.24	15*	7.95 (s)	0.34
16	7.80 (s)	-0.06	16*	7.70 (s)	0.04
17	4.55 (d, J = 8.0 Hz)	2.51	17*	7.43	-0.37
18	5.50 (d, J = 8.1 Hz)	1.72	18*	7.10	0.12
19	5.38 (d, J = 8.1 Hz)	1.68	19*	7.10 (d, J = 8.2 Hz)	-0.04
20	4.28 (d, J = 8.0 Hz)	2.34	20*	5.90 (d, J = 8.1 Hz)	0.72
21	6.30 (d, J = 7.9 Hz)	1.26	21*	7.05	0.51
22	6.87 (d, J = 7.9 Hz)	0.35	22*	7.15	0.07
24	3.09 (s)	0.39	24*	3.07 (s)	0.41
25*	6.65 (d, J = 16.0 Hz)	0.21	26*	5.35	2.18

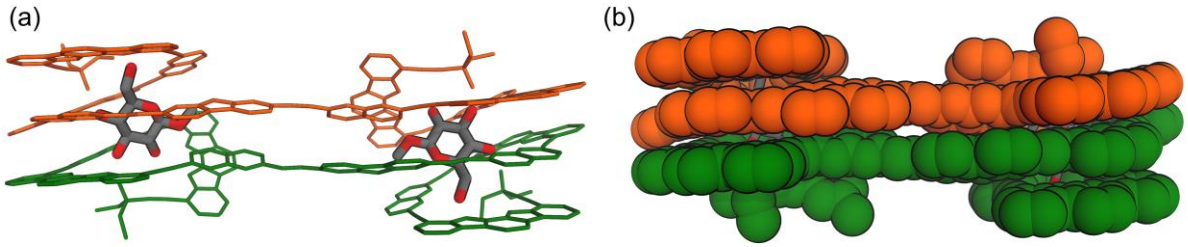

Fig. S8 (a) Tube and (b) space-filling representations of energy-minimized structure of (**1**-*MP*)$_2$⊃(me-β-D-glc)$_2$ (MacroModel 9.1, MMFFs force field, $CHCl_3$ phase).

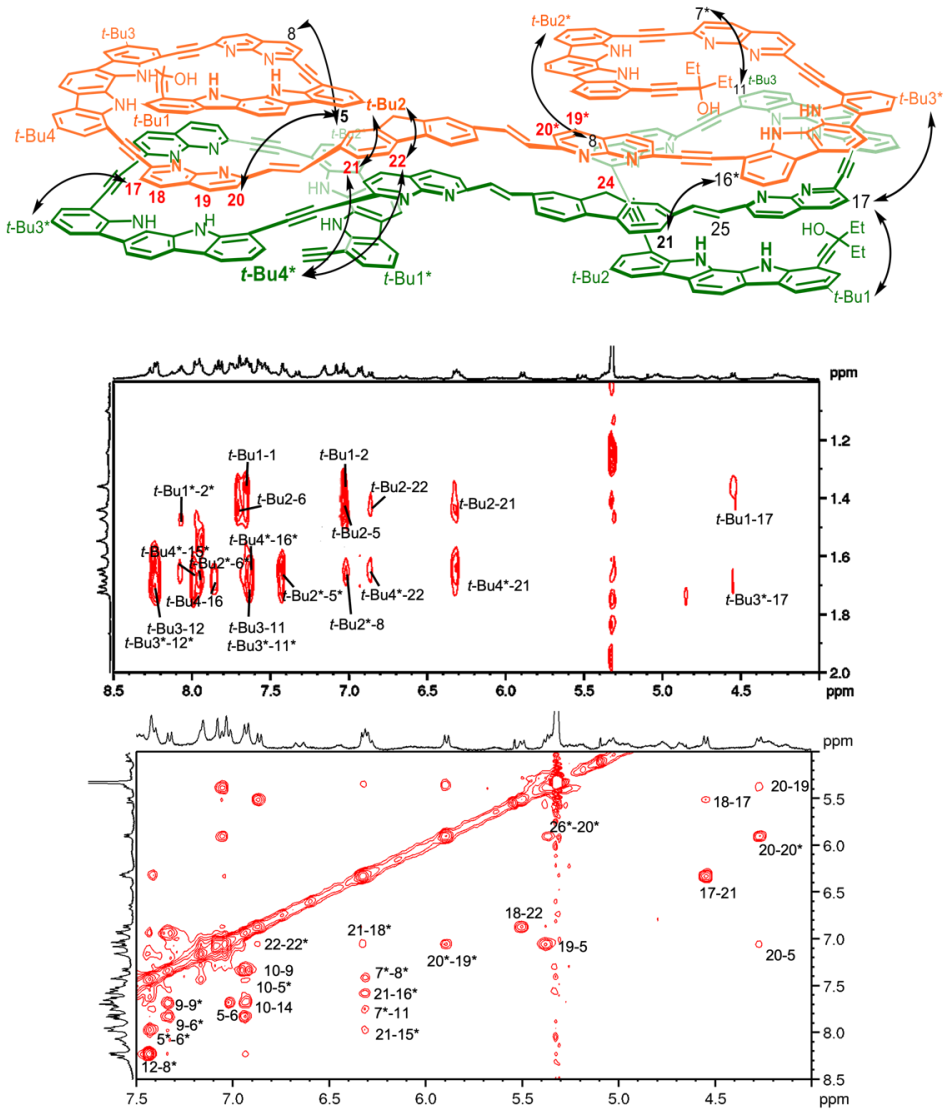

Fig. S9 Partial ^{1}H-^{1}H ROESY spectrum (400 MHz, 25 °C, mixing time: 400 ms) of (**1**-*MP*)$_2$⊃(me-β-D-glc)$_2$ (4.0 mM) in 3% (v/v) DMSO-d_6/CD_2Cl_2.

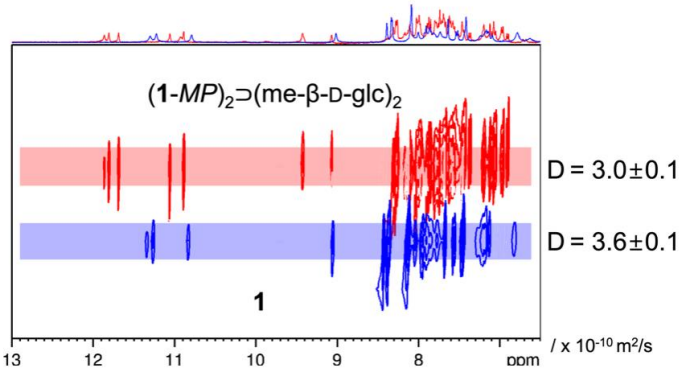

Fig. S10 Partial DOSY spectra of **1** in the absence and presence of me-β-D-glc (2 mM) in 2% (v/v) DMSO-d_6/CD_2Cl_2.

2.3 ^{1}H NMR spectra of **2**, and (**2**-*MP*)$_2$⊃(me-β-D-glc)$_2$

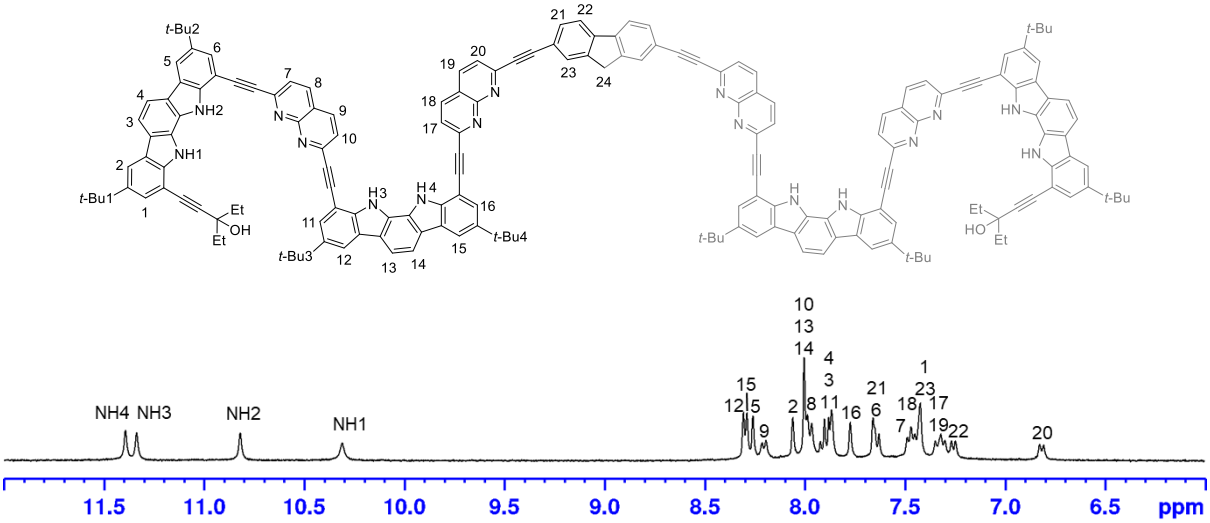

Fig. S11 Partial ^{1}H NMR spectrum (400 MHz, 25 °C) of **2** (2 mM) in 5 % (v/v) DMSO-d_6/CD_2Cl_2.

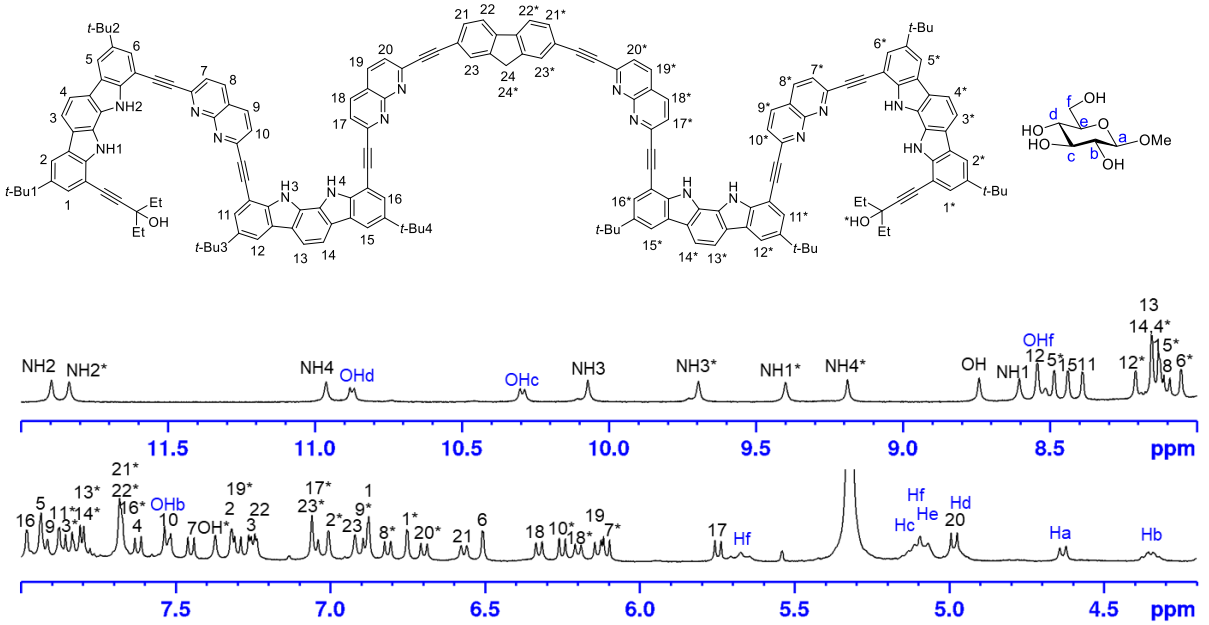

Fig. S12 Partial ^{1}H NMR spectrum (400 MHz, 25 °C) of (**2**-*MP*)$_2$⊃(me-β-D-glc)$_2$ (2 mM) in 5% (v/v) DMSO-d_6/CD_2Cl_2. Me-β-D-glc signals are depicted in blue.

Table S3 ^{1}H NMR chemical shifts (400 MHz, 25 °C) of (**2**-*MP*)$_2$⊃(me-β-D-glc)$_2$ (2 mM) in 5% (v/v) DMSO-d_6/CD_2Cl_2 and their differences between free **2**.

(**2**-*MP*)$_2$⊃(me-β-D-glc)$_2$			(**2**-*MP*)$_2$⊃(me-β-D-glc)$_2$		
atom	δ (ppm)	δ (free) − δ (complex)	atom	δ (ppm)	δ (free) − δ (complex)
1	6.88 (s)	0.54	1*	6.75 (s)	0.67
2	7.32 (s)	0.74	2*	7.00 (s)	1.06
3	7.25 (d, J = 8.2 Hz)	0.62	3*	7.84 (d, J = 8.2 Hz)	0.03
4	7.62 (d, J = 8.1 Hz)	0.29	4*	8.15 (s)	-0.24
5	7.93 (s)	0.33	5*	8.48 (s)	-0.22
6	6.51 (s)	1.15	6*	8.05 (s)	-0.39
7	7.45 (d, J = 8.1 Hz)	0.03	7*	6.11 (d, J = 8.0 Hz)	1.37
8	8.10 (d, J = 8.1 Hz)	-0.12	8*	6.81 (d, J = 8.1 Hz)	1.17
9	7.92 (d, J = 8.2 Hz)	0.28	9*	6.88 (d, J = 8.0 Hz)	1.32
10	7.53 (d, J = 8.1 Hz)	0.47	10*	6.25 (d, J = 8.1 Hz)	1.75
11	8.39 (s)	-0.53	11*	7.88 (d, J = 1.5 Hz)	-0.02
12	8.54 (s)	-0.24	12*	8.21 (s)	0.09
13	8.15 (s)	-0.15	13*	7.78 (d, J = 8.2 Hz)	0.22
14	8.15 (s)	-0.15	14*	7.82 (d, J = 8.1 Hz)	0.18
15	8.44 (s)	-0.15	15*	8.13 (s)	0.16
16	7.98 (s)	-0.21	16*	7.68 (s)	0.09
17	5.75 (d, J = 8.0 Hz)	1.56	17*	7.05 (d, J = 8.0 Hz)	0.26
18	6.32 (d, J = 8.0 Hz)	1.14	18*	6.20 (d, J = 8.1 Hz)	1.26
19	6.13 (d, J = 8.1 Hz)	1.17	19*	7.30 (d, J = 8.0 Hz)	0.00
20	4.98 (d, J = 8.0 Hz)	1.84	20*	6.70 (d, J = 8.0 Hz)	0.12
21	6.57 (d, J = 7.4 Hz)	1.06	21*	7.68 (br)	-0.05
22	7.25 (d, J = 7.4 Hz)	0.00	22*	7.68 (br)	-0.43
23	6.92 (s)	0.50	23*	7.06 (s)	0.36
24	3.12 (s)	0.53	24*	3.07 (s)	0.56
OMe	0.95 (s)		Ha	4.63 (d, J = 8.0 Hz)	
OHb	7.53 (d, J = 6.0 Hz)		Hb	4.34	
OHc	10.29 (d, J = 6.2 Hz)		Hc	5.13	
OHd	10.87 (d, J = 5.8 Hz)		Hd	4.96	
OHf	8.51 (s)		He	5.07	
Hf	5.67		Hf	5.09	

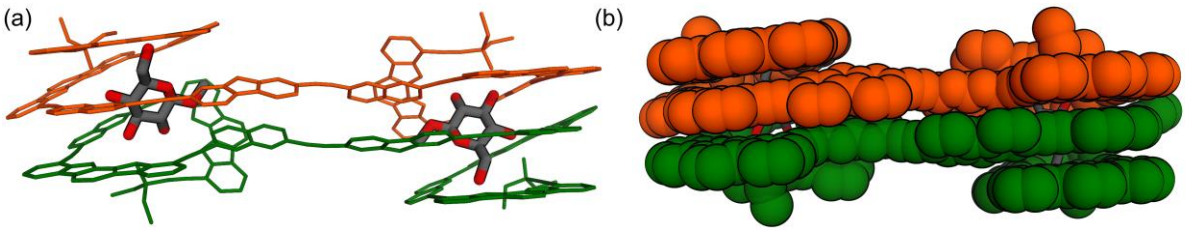

Fig. S13 (a) Tube and (b) space-filling representations of energy-minimized structure of (**2**-*MP*)$_2$⊃(me-β-D-glc)$_2$ (MacroModel 9.1, MMFFs force field, $CHCl_3$ phase).

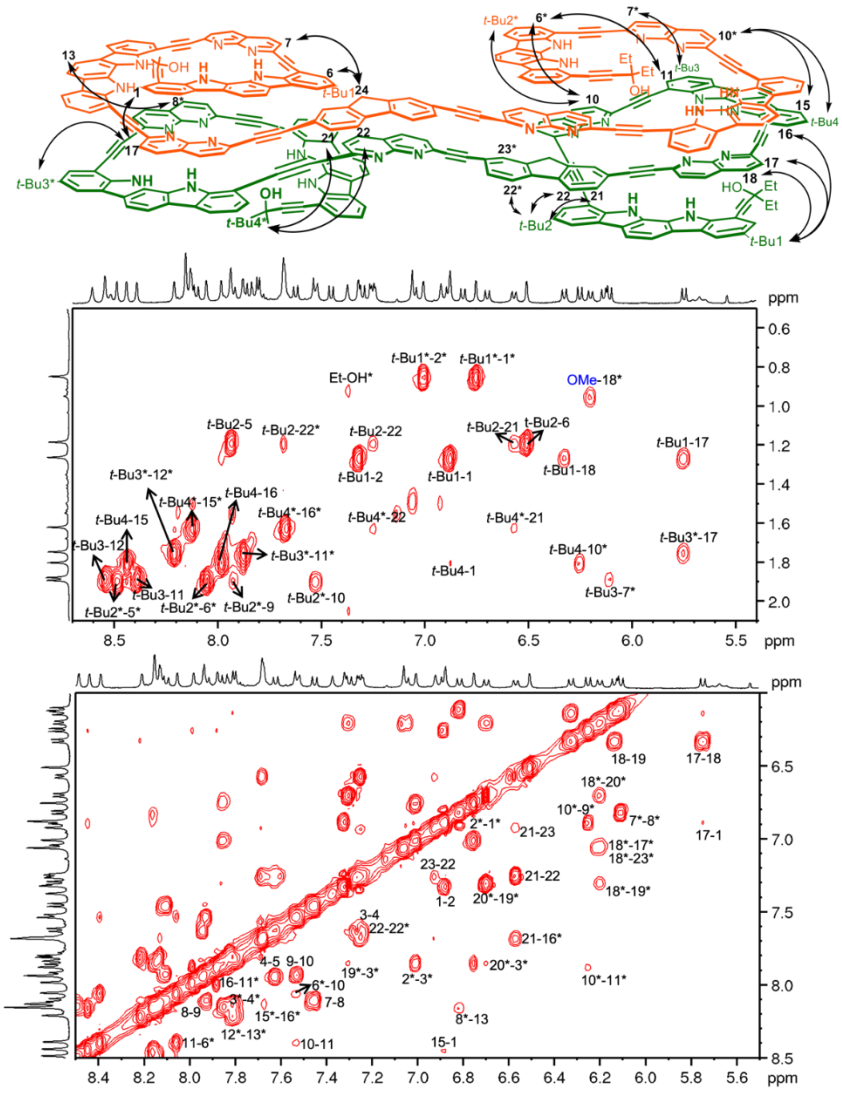

Fig. S14 Partial ^{1}H-^{1}H ROESY spectrum (400 MHz, 25 °C, mixing time: 400 ms) of (**2**-*MP*)$_2$⊃(me-β-D-glc)$_2$ (4.0 mM) in CD_2Cl_2.

2.4 ^{1}H NMR spectra in the U-tube transport experiments

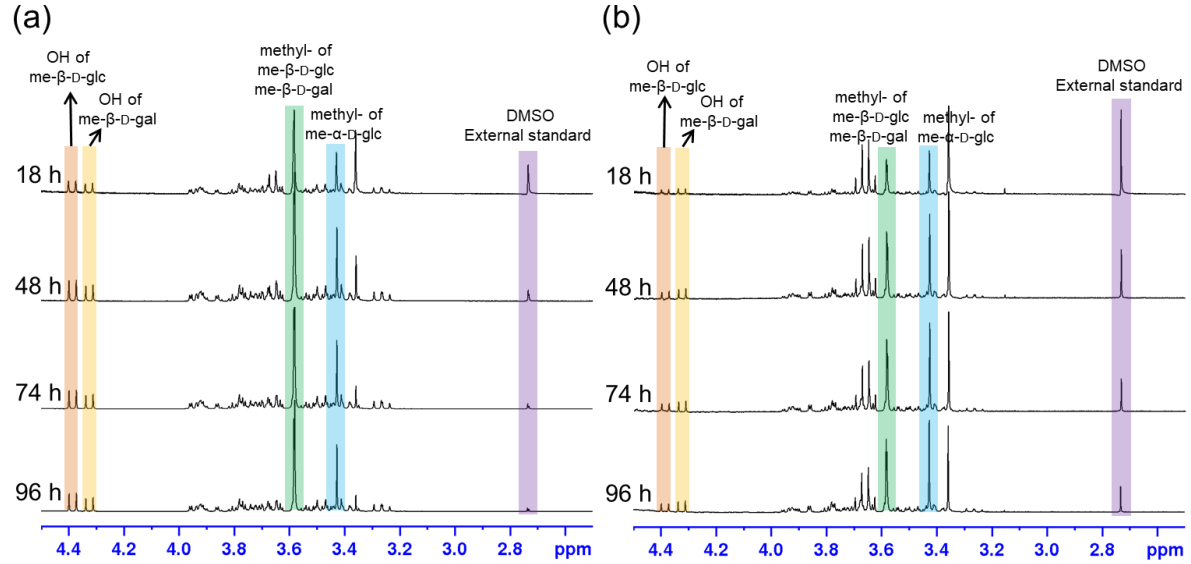

Fig. S15 Time-dependent ^{1}H NMR spectra (400 MHz, D_2O, 25 °C) of the receiving phase in U-tube transport experiments: (a) in the presence or receptor **2** (3 mM) or (b) in its absence.

3. CD studies

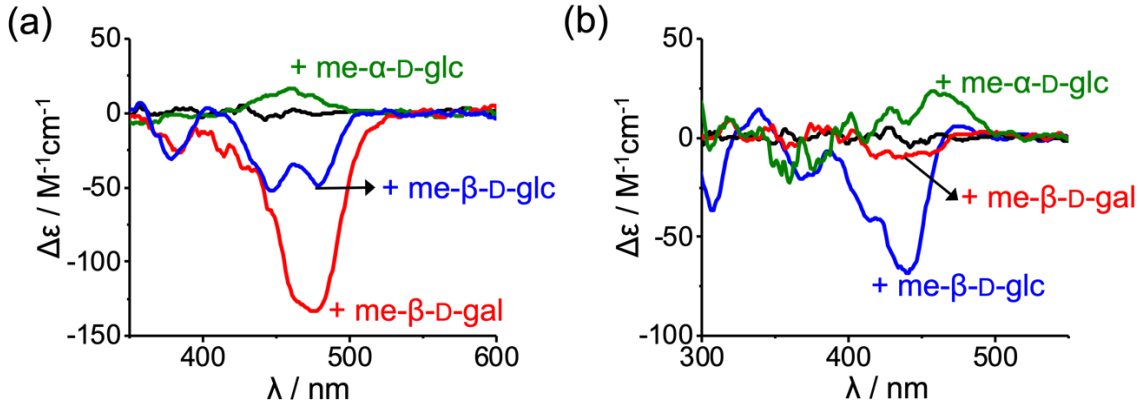

Fig. S16 CD spectra of (a) **1** and (b) **2** (2.00×10^{-5} M) in the absence and presence of guests (200 equiv) in 5% (v/v) DMSO/CH_2Cl_2 at 25 °C.

4. Binding studies

4.1 ^{1}H NMR titrations

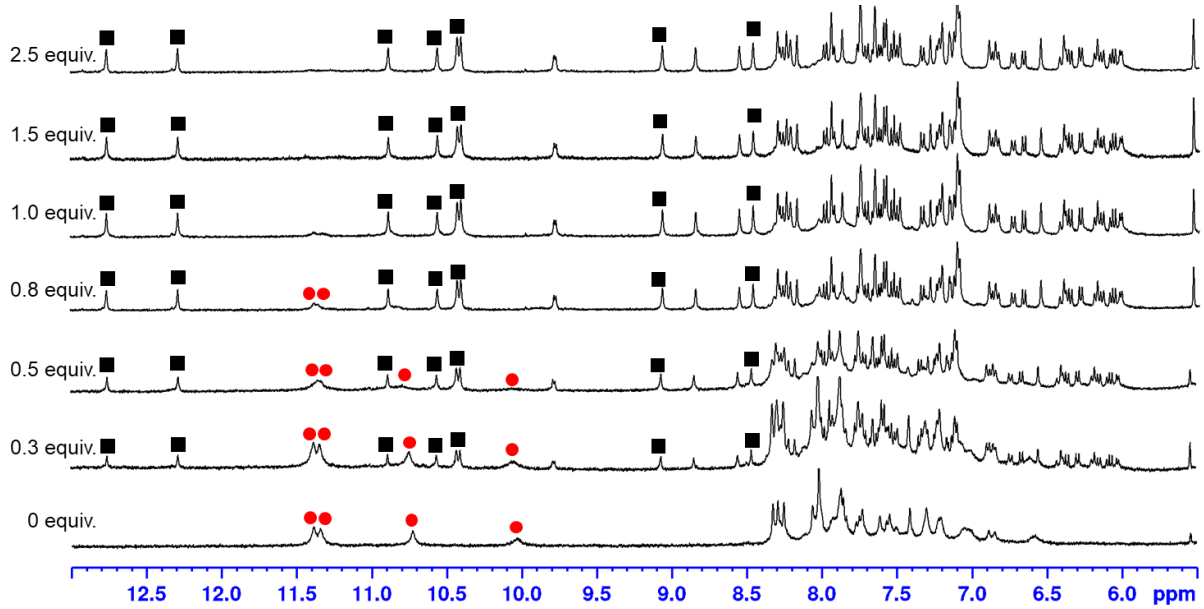

Fig. S17 Partial ^{1}H NMR spectral changes of **1** (1.50 mM, 25 ± 1 °C) with increasing the amount of me-β-D-gal in 5% (v/v) DMSO-d_6/CD_2Cl_2 (containing ca. 0.05 % water). The NH signals of free **1** and its 2:2 complex are marked with red circles and black squares, respectively.

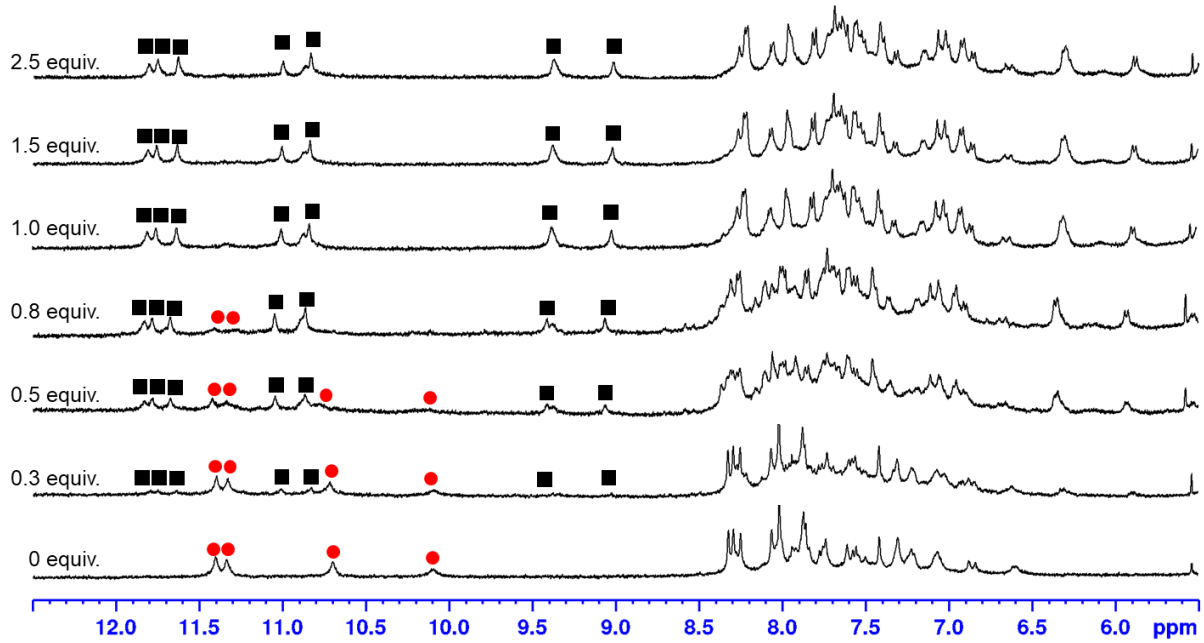

Fig. S18 Partial ^{1}H NMR spectral changes of **1** (1.50 mM, 25 ± 1 °C) with increasing the amount of me-β-D-glc in 5% (v/v) DMSO-d_6/CD_2Cl_2 (containing ca. 0.05 % water). The NH signals of free **1** and its 2:2 complex are marked with red circles and black squares, respectively.

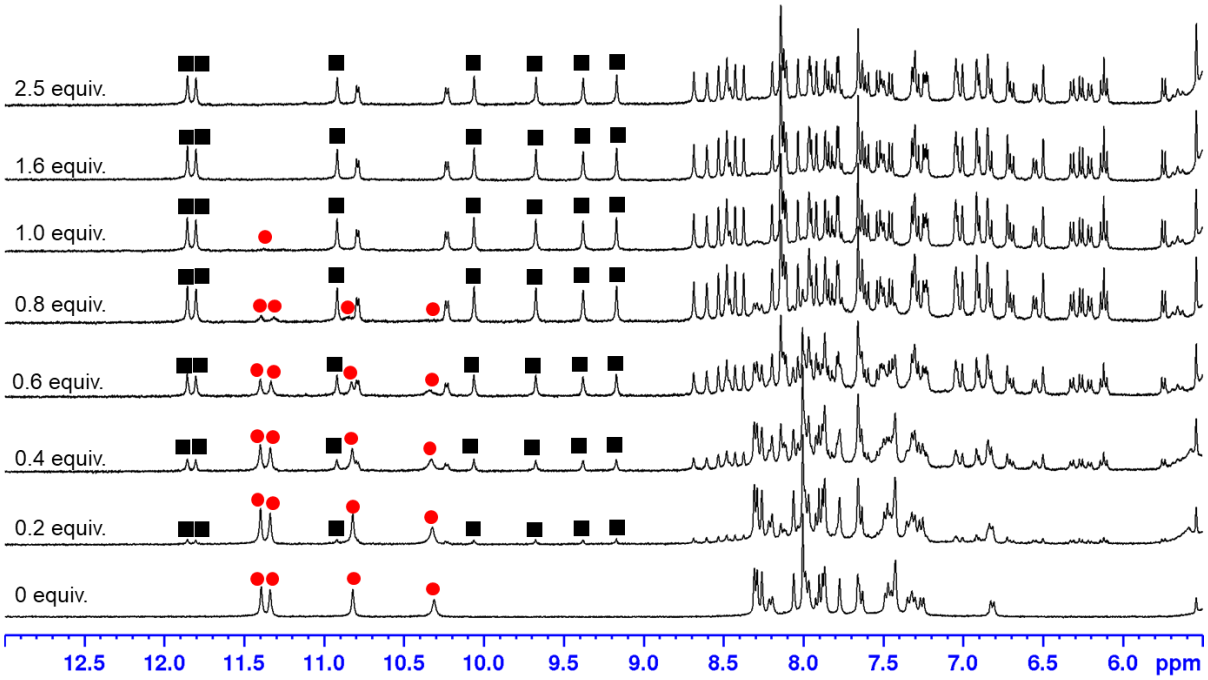

Fig. S19 Partial ^{1}H NMR spectral changes of **2** (1.50 mM, 25 ± 1 °C) with increasing the amount of me-β-D-glc in 5% (v/v) DMSO-d_6/CD_2Cl_2 (containing ca. 0.05 % water). The NH signals of free **2** and its 2:2 complex are marked with red circles and black squares, respectively.

4.2 Isothermal titration calorimetry (ITC) experiments

The Hypcal software program analyzed the ITC experimental data using a 2:2 binding model, yielding values for ΔH and *K*. The Gibbs free energy change (ΔG) was subsequently derived from *K*, allowing for the calculation of the entropy change (ΔS) based on the relationship between ΔH and ΔG (common thermodynamic equation).

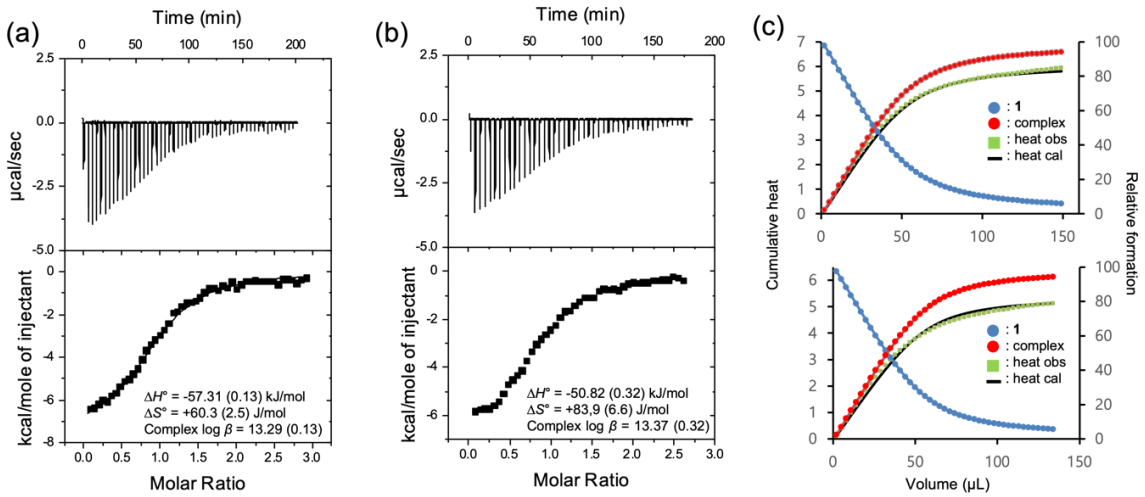

Fig. S20 (a,b) Experimental ITC measurements and binding isotherms of **1** (1.50×10^{-4} M) with me-β-D-glc (4.00×10^{-3} M) in 5 % (v/v) DMSO/CH_2Cl_2 (containing ca. 0.05 % water) at 22 ± 1 °C. (c) Relative distributions of unbound **1** and its complex, along with experimental and theoretical cumulative heat profiles. In (c), the top represents (a), and the bottom (b).

Table S4 Thermodynamic parameters between **1** and me-β-D-glc in 5 % (v/v) DMSO/CH_2Cl_2 at 22 °C.

	L	$\Delta G°$ (kJ·mol^{-1})	$\Delta H°$ (kJ·mol^{-1})	$T\Delta S°$ (kJ·mol^{-1})
(a)	13.3	−75.1	−57.3	+17.8
(b)	13.4	−75.6	−52.8	+22.8

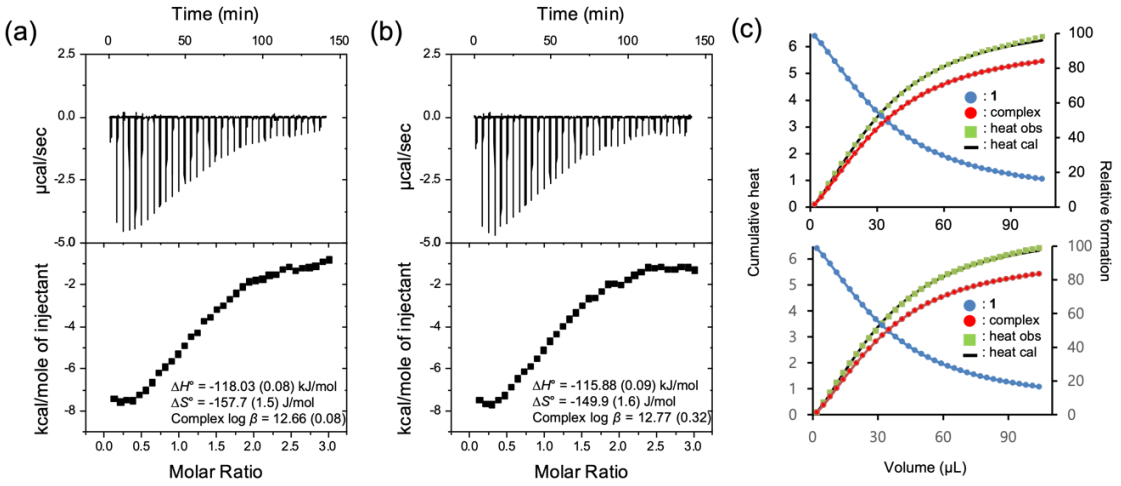

Fig. S21 (a,b) Experimental ITC measurements and binding isotherms of **1** (9.00×10^{-5} M) with me-β-D-gal (4.00×10^{-3} M) in 5 % (v/v) DMSO/CH_2Cl_2 (containing ca. 0.05 % water) at 22 ± 1 °C. (c) Relative distributions of unbound **1** and its complex, along with experimental and theoretical cumulative heat profiles. In (c), the top represents (a), and the bottom (b).

Table S5 Thermodynamic parameters between **1** and me-β-D-gal in 5 % DMSO/CH_2Cl_2 at 22 °C.

	L	$\Delta G°$ (kJ·mol^{-1})	$\Delta H°$ (kJ·mol^{-1})	$T\Delta S°$ (kJ·mol^{-1})
(a)	12.7	−71.5	−118.0	−46.5
(b)	12.8	−71.7	−115.9	−44.2

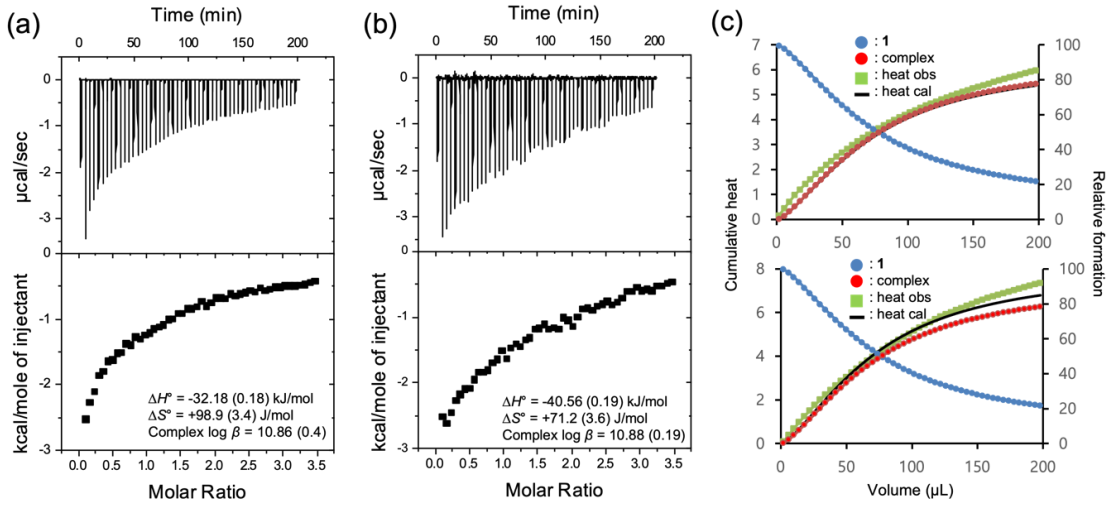

Fig. S22 (a,b) Experimental ITC measurements and binding isotherms of **1** (3.00×10^{-4} M) with me-α-D-glc (7.00×10^{-3} M) in 5 % (v/v) DMSO/CH_2Cl_2 (containing ca. 0.05 % water) at 22 ± 1 °C. (c) Relative distributions of unbound **1** and its complex, along with experimental and theoretical cumulative heat profiles. In (c), the top represents (a), and the bottom (b).

Table S6 Thermodynamic parameters between **1** and me-α-D-glc in 5 % (v/v) DMSO/CH_2Cl_2 at 22 °C.

	L	$\Delta G°$ (kJ·mol^{-1})	$\Delta H°$ (kJ·mol^{-1})	$T\Delta S°$ (kJ·mol^{-1})
(a)	10.9	−61.2	−32.2	+29.0
(b)	10.9	−61.6	−40.6	+21.0

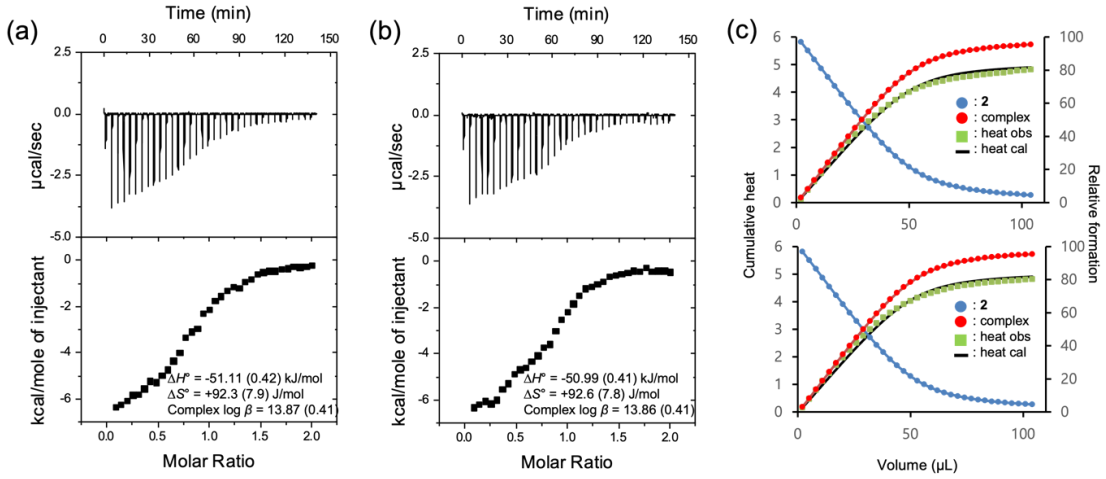

Fig. S23 (a,b) Experimental ITC measurements and binding isotherms of **2** (1.50×10^{-4} M) with me-β-D-glc (4.00×10^{-3} M) in 5 % (v/v) DMSO/CH_2Cl_2 (containing ca. 0.05 % water) at 22 ± 1 °C. (c) Relative distribution of unbound **2** and its complex, along with experimental and theoretical cumulative heat profiles. In (c), the top represents (a), and the bottom (b).

Table S7 Thermodynamic parameters between **2** and me-β-D-glc in 5 % DMSO/CH_2Cl_2 at 22 °C.

	L	$\Delta G°$ (kJ·mol^{-1})	$\Delta H°$ (kJ·mol^{-1})	$T\Delta S°$ (kJ·mol^{-1})
(a)	13.9	−78.3	−51.1	+27.2
(b)	13.9	−78.3	−51.0	+27.3

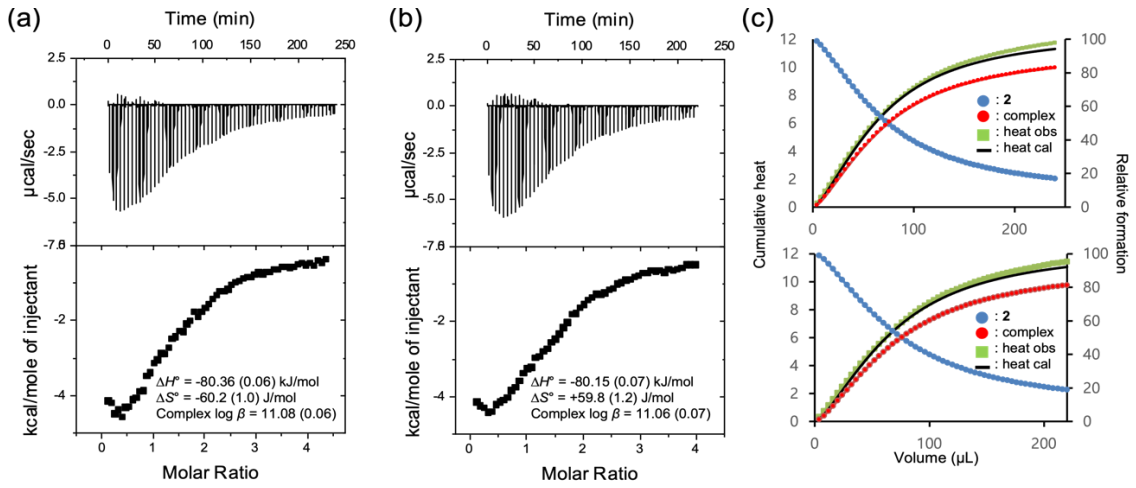

Fig. S24 (a,b) Experimental ITC measurements and binding isotherms of **2** (2.50×10^{-4} M) with me-β-D-gal (6.00×10^{-3} M) in 5 % (v/v) DMSO/CH_2Cl_2 (containing ca. 0.05 % water) at 22 ± 1 °C. (c) Relative distribution of unbound **2** and its complex, along with experimental and theoretical cumulative heat profiles. In (c), the top represents (a), and the bottom (b).

Table S8 Thermodynamic parameters between **2** and me-β-D-gal in 5 % DMSO/CH_2Cl_2 at 22 ± 1 °C.

	L	$\Delta G°$ (kJ·mol^{-1})	$\Delta H°$ (kJ·mol^{-1})	$T\Delta S°$ (kJ·mol^{-1})
(a)	11.1	−62.6	−80.4	−17.8
(b)	11.1	−62.6	−80.2	−17.6

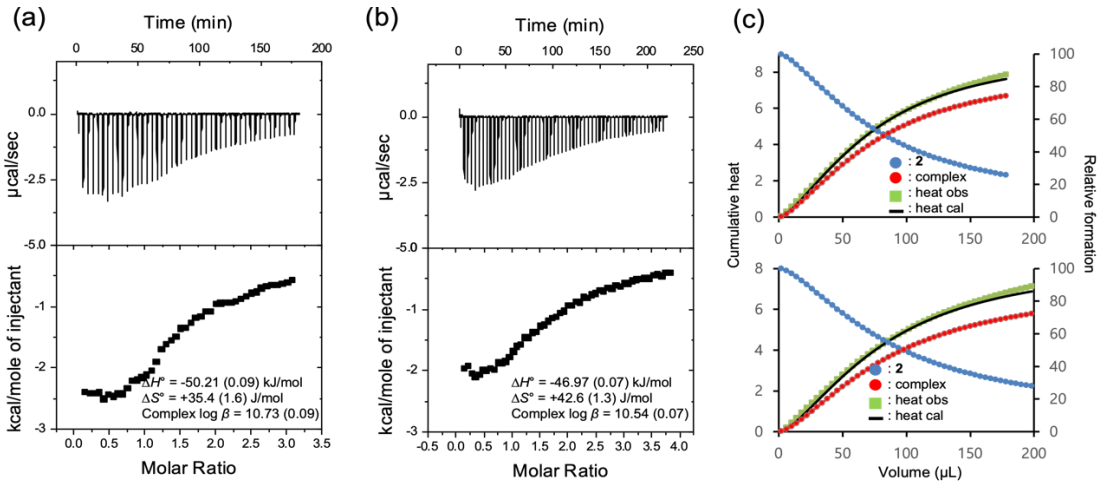

Fig. S25 (a,b) Experimental ITC measurements and binding isotherms of **2** (3.00×10^{-4} M) with me-α-D-glc (7.00×10^{-3} M) in 5 % (v/v) DMSO/CH_2Cl_2 (containing ca. 0.05 % water) at 22 ± 1 °C. (c) Relative distribution of unbound **2** and its complex, along with experimental and theoretical cumulative heat profiles. In (c), the top represents (a), and the bottom (b).

Table S9. Thermodynamic parameters between **2** and me-α-D-glc in 5 % DMSO/CH_2Cl_2 at 22 ± 1 °C.

	L	$\Delta G°$ (kJ·mol^{-1})	$\Delta H°$ (kJ·mol^{-1})	$T\Delta S°$ (kJ·mol^{-1})
(a)	10.7	−60.6	−50.2	+10.4
(b)	10.5	−59.6	−47.0	+12.6

5. Mass spectra

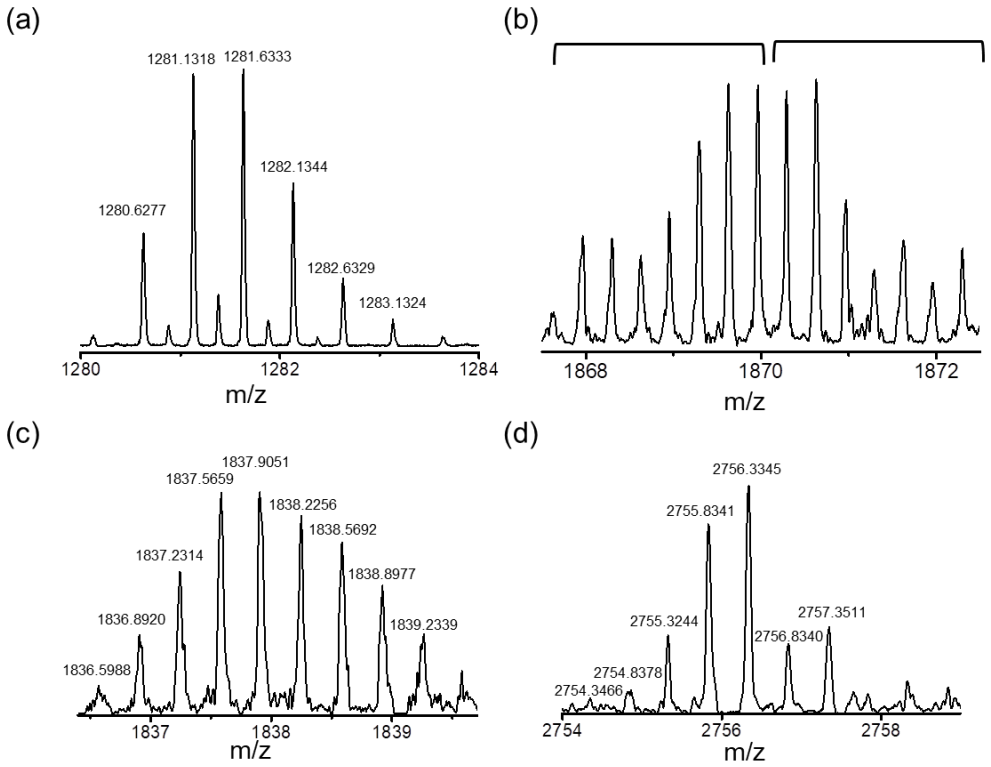

Fig. S26 ESI-MS isotopic distribution of (a) $[\mathbf{1}+2H]^{2+}$, (b) $[(\mathbf{1}\text{-}MM)_2\supset(\text{me-}\beta\text{-D-gal}\cdot 2H_2O)_2+2H+Na]^{3+}$ and $[(\mathbf{1}\text{-}MM)_2\supset(\text{me-}\beta\text{-D-gal}\cdot 2H_2O)_2+H+2Na-H_2O]^{3+}$, (c) $[(\mathbf{1}\text{-}MP)_2\supset(\text{me-}\beta\text{-D-glc})_2+3H]^{3+}$, and (d) $[(\mathbf{1}\text{-}MP)_2\supset(\text{me-}\beta\text{-D-glc})_2+2H]^{2+}$.

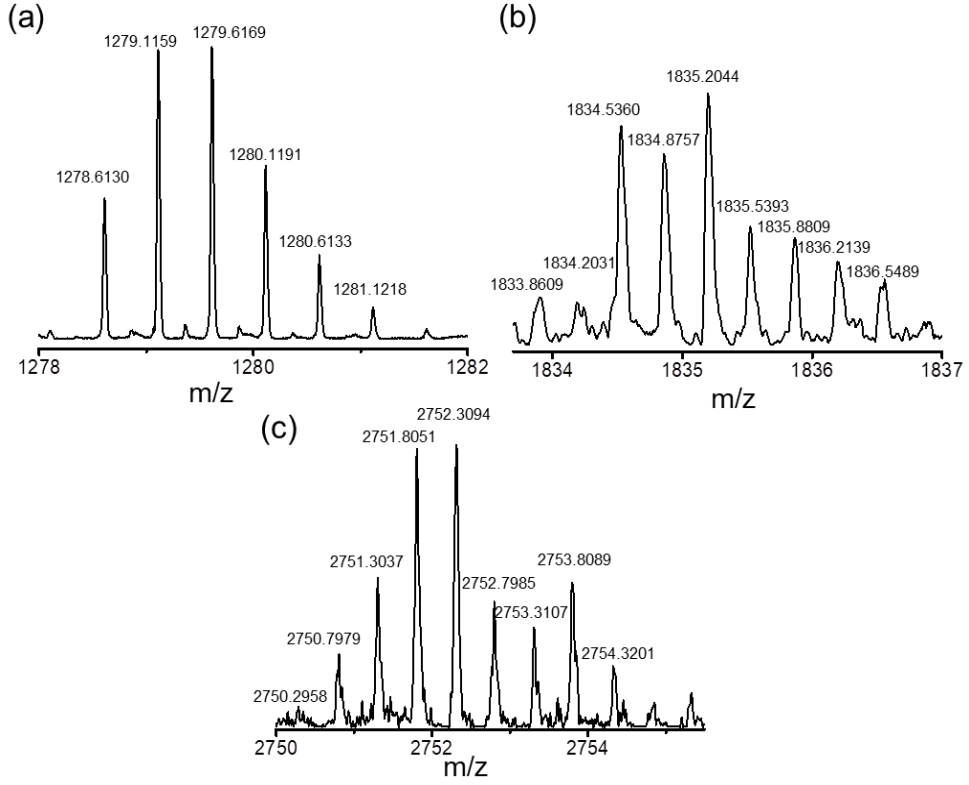

Fig. S27 ESI-MS isotopic distribution of (a) $[\mathbf{2}+2H]^{2+}$, (b) $[(\mathbf{2}\text{-}MP)_2\supset(\text{me-}\beta\text{-D-glc})_2+3H]^{3+}$, and (c) $[(\mathbf{2}\text{-}MP)_2\supset(\text{me-}\beta\text{-D-glc})_2+2H]^{2+}$.

6. ^{1}H, ^{13}C NMR spectra of new compounds

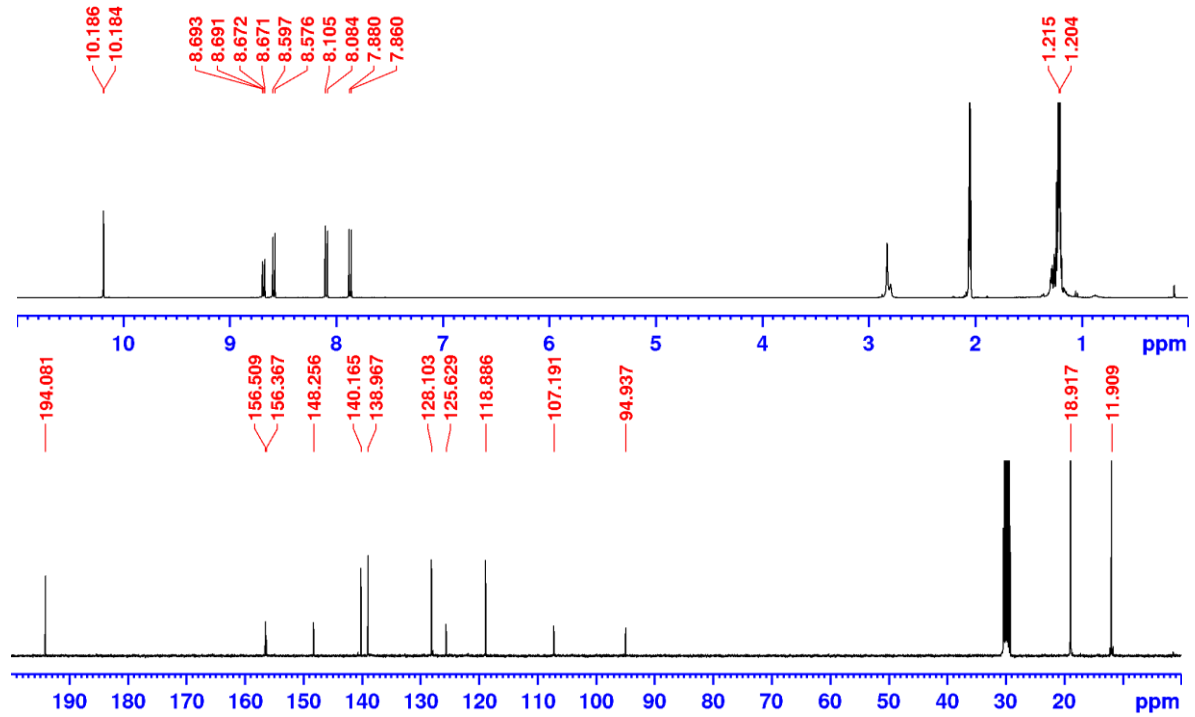

Fig. S28 ^{1}H and ^{13}C spectra of compound **5** (Acetone-d_6, 25 °C).

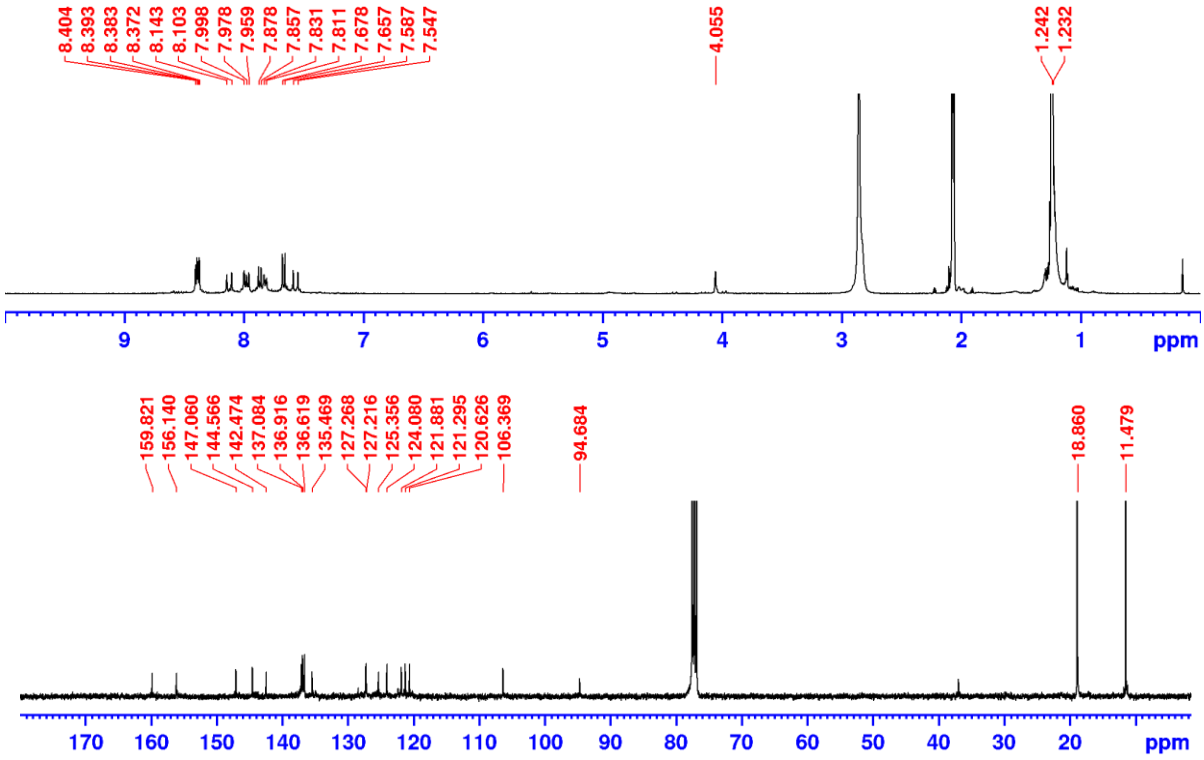

Fig. S29 ^{1}H (Acetone-d_6) and ^{13}C ($CDCl_3$) spectra of compound **7** (25 °C).

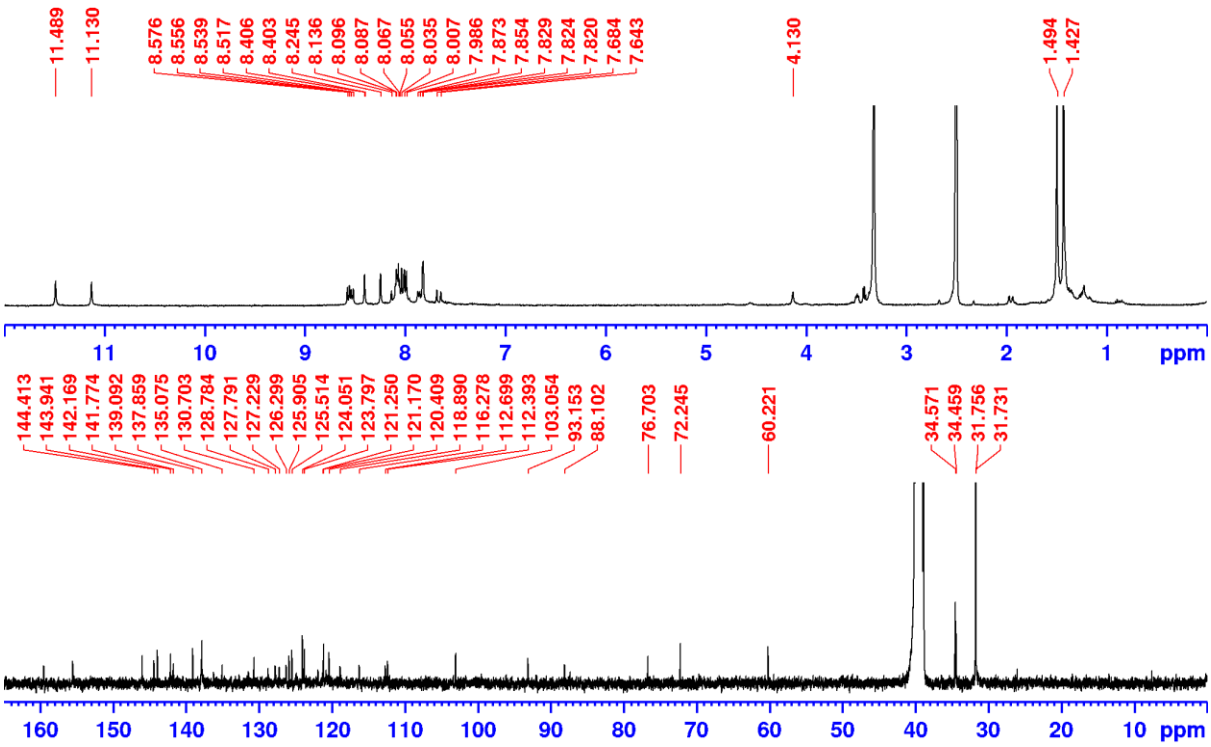

Fig. S30 ^{1}H and ^{13}C spectra of compound **9** (DMSO-d_6, 25 °C).

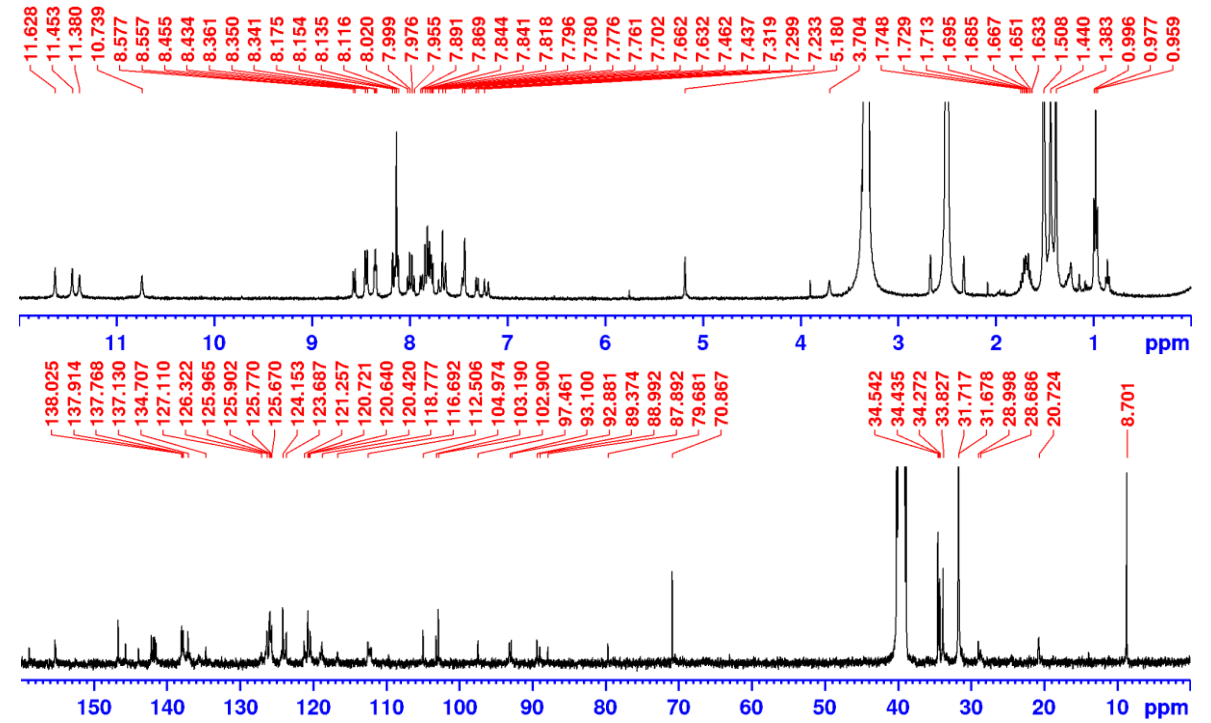

Fig. S31 ^{1}H and ^{13}C spectra of compound **1** (DMSO-d_6, 25 °C).

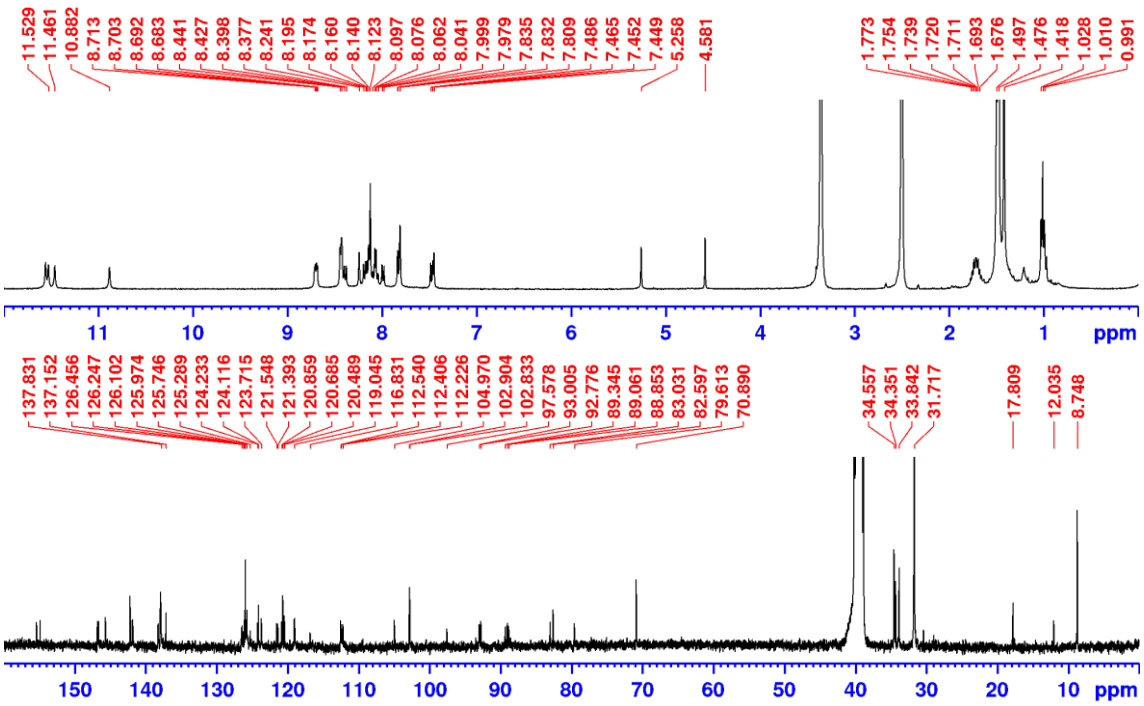

Fig. S32 ^{1}H and ^{13}C spectra of compound **12** (DMSO-d_6, 25 °C).

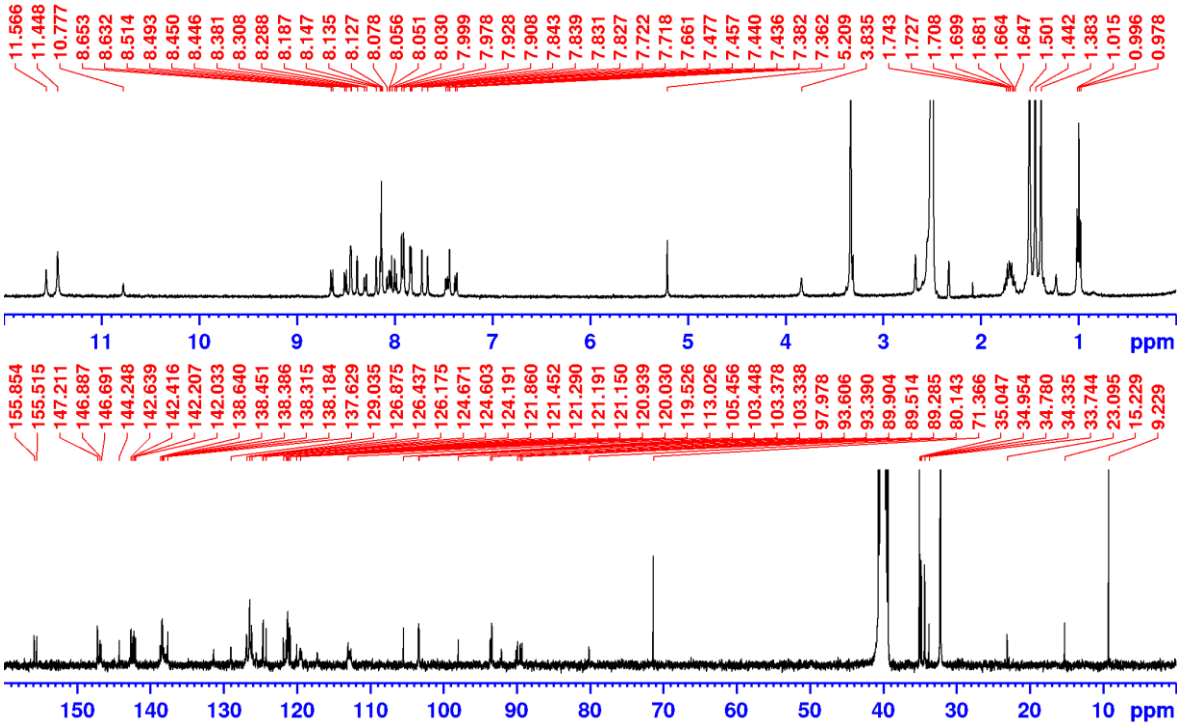

Fig. S33 ^{1}H and ^{13}C spectra of compound **2** (DMSO-d_6, 25 °C).

7. References

S1. R. Rosin, W. Seichter, A. Schwarzer and M. Mazik, *Eur. J. Org. Chem. 2017*, 6038–6051.

S2. D. Wang, M. V. Ivanov, D. Kokkin, J. Loman, J.-Z. Cai, S. A. Reid and R. Rathore, *Angew. Chem. Int. Ed., 2018*, **57**, 8189–8193.

S3. K.-J. Chang, D. Moon, M. S. Lah and K.-S. Jeong, *Angew. Chem. Int. Ed. 2005*, **44**, 7926–7929.

S4. K. M. Kim, G. Song, S. Lee, H.-G. Jeon, W. Chae and K.-S. Jeong, *Angew. Chem. Int. Ed. 2020*, **59**, 22475–22479.

S5. G. Song and K.-S. Jeong, *ChemPlusChem 2020*, **85**, 2475–2481.